Journal of Theoretical Biology 378 (2015) 12–30

Contents lists available at ScienceDirect

Journal of Theoretical Biology

journal homepage: www.elsevier.com/locate/yjtbi

The impact of environmental toxins on predator–prey dynamics

Qihua Huang [a,*], Hao Wang [a], Mark A. Lewis [a,b]

[a] Center for Mathematical Biology, Department of Mathematical and Statistical Sciences, University of Alberta, Edmonton, Alberta, Canada T6G 2G1
[b] Department of Biological Sciences, University of Alberta, Edmonton, Alberta, Canada T6G 2G1

HIGHLIGHTS

- We develop a toxin-dependent predator–prey model.
- We examine how environmental toxin levels alter the balance of the classical predator–prey dynamics.
- We investigate the effect of methylmercury on rainbow trout and its prey.

ARTICLE INFO

Article history:
Received 21 December 2014
Received in revised form
9 April 2015
Accepted 15 April 2015
Available online 25 April 2015

Keywords:
Toxin
Predator–prey model
Bifurcation
Methylmercury
Rainbow trout

ABSTRACT

Predators and prey may be simultaneously exposed to environmental toxins, but one may be more susceptible than the other. To study the effects of environmental toxins on food web dynamics, we develop a toxin-dependent predator–prey model that combines both direct and indirect toxic effects on two trophic levels. The direct effects of toxins typically reduce organism abundance by increasing mortality or reducing fecundity. Such direct effects, therefore, alter both bottom-up food availability and top-down predatory ability. However, the indirect effects, when mediated through predator–prey interactions, may lead to counterintuitive effects. This study investigates how the balance of the classical predator–prey dynamics changes as a function of environmental toxin levels. While high toxin concentrations are shown to be harmful to both species, possibly leading to extirpation of both species, intermediate toxin concentrations may affect predators disproportionately through biomagnification, leading to reduced abundance of predators and increased abundance of the prey. This counterintuitive effect significantly increases biomass at the lower trophic level. Environmental toxins may also reduce population variability by preventing populations from fluctuating around a coexistence equilibrium. Finally, environmental toxins may induce bistable dynamics, in which different initial population levels produce different long-term outcomes. Since our toxin-dependent predator–prey model is general, the theory developed here not only provides a sound foundation for population or community effects of toxicity, but also could be used to help develop management strategies to preserve and restore the integrity of contaminated habitats.

1. Introduction

There is increasing global concern over the effects of anthropogenic and natural environmental toxins on ecosystem health. Industrial toxins are one of the leading causes of pollution worldwide. Industrial toxins may arise as a result of air emissions, water releases, water seepage, air deposition or disposal and leaching of solid waste. Toxins of concern may also be transported through natural systems as a result of weathering or leaching. The US Environmental Protection Agency has designated 126 priority pollutants (U.S. National Archives and Records Administration, 2013) and the Canadian Council of Ministers of the Environment has a list of priority chemicals of concern for the protection of aquatic life (Canadian Council of Ministers of the Environment, 2003a). These priority substances include metals and organic compounds.

The combination of natural and anthropogenic sources of toxins present challenges with respect to the protection of local freshwater resources. To protect ecological environments and aquatic species, it is necessary to assess the risk to aquatic organisms exposed to toxins, and find relevant factors that determine the persistence and extirpation of organisms. Kooijman and Bedaux (1996) describe how the no-effect concentration can be estimated from data of standardized aquatic toxicity tests: acute and chronic survival, body growth, reproduction, and population growth.

* Corresponding author. Tel.: +1 7804920147.
E-mail addresses: qihua@ualberta.ca (Q. Huang), hao8@ualberta.ca (H. Wang), mark.lewis@ualberta.ca (M.A. Lewis).

http://dx.doi.org/10.1016/j.jtbi.2015.04.019
0022-5193/

Over the past several decades, mathematical models have been widely applied to perform chemical risk assessments on all levels of biological hierarchy, from cells to organs to organisms to populations to entire ecosystems. These models include population models (scalar abundance, life history, individual-based, and metapopulation), ecosystem models (food-web, aquatic and terrestrial), landscape models, and toxicity-extrapolation models (Bartell et al., 2003; Galic et al., 2010; Pastorok et al., 2001, 2003). The selection of specific models for addressing an ecological risk issue depends on the habitat; endpoints and chemicals of interest; the balance between model complexity and availability of data; the degree of site specificity of available models; and, the risk issue (Pastorok et al., 2001). A comprehensive review of the realism, relevance, and applicability of different types of models from the perspective of assessing risks posed by toxic chemicals is provided by Bartell et al. (2003) and Pastorok et al. (2001).

In practice, toxin-dependent individual-based models and matrix population models are widely used to evaluate the ecological significance of observed or predicted effects of toxic chemicals on individual organisms and population dynamics. Despite the nonlinear dynamical nature of population-toxin interactions, our search of the literature shows that relatively few differential equation models have been developed to describe population-toxin interactions (but see Freedman and Shukla, 1991; Hallam and Clark, 1983; Hallam et al., 1983; Luna and Hallam, 1987; Thieme, 2003; Thomas et al., 1996). For those models that do exist, interactions are usually described by a system, which contains components representing the population density, the concentration of toxin in an organism, and the environmental concentration of toxin.

Recently, we developed a toxin-dependent model given by a system of differential equations, to describe the impact of contaminants on fish population dynamics (Huang et al., 2013). Because the concentration of toxin in the environment is not affected significantly by mortality or metabolic processes of population, our toxin-dependent model focused on the impact of toxin on the population and ignores the influence of the population on the concentration of toxin in the environment. The concentration of toxin in the environment hence was treated as a parameter. The model was connected to literature-sourced experimental data via model parameterization of the toxic effects of methylmercury on rainbow trout (*Oncorhynchus mykiss*). The parameter estimates were then used to illustrate the long-term behavior of rainbow trout population. The numerical results provided threshold values of concentration of methylmercury in the environment to maintain populations and prevent extirpation.

It is significant that all above-mentioned differential equation models are single-species models in which populations are assumed to take up toxin only from exposure to the environment. However, it is well recognized that the primary route of toxin uptake in higher-trophic level organisms (predators) is via food ingestion. As one organism eats another, it also eats the pollutants in its prey. The higher up the food chain, the more the pollutants that are eaten and stored. This build-up of toxic pollutants is referred to as bioaccumulation (Arnot and Gobas, 2004; Mackay and Fraser, 2000; Mathew et al., 2008). Bioaccumulation means that the nonlinear effects observed in ecosystems cannot often be described or understood through studying species individually because food web interactions must be considered (e.g., Kidd et al., 2007). A review on bioaccumulation criteria and methods is provided in Gobas et al. (2009). Moreover, Kelly et al. (2007) and Thomann (1989) developed bioaccumulation models.

In this work, we evaluate the flow of contaminants through a simple aquatic food web and study how the transfer of contaminants between trophic levels affects food web dynamics. We do this by extending the single-species toxin-dependent model in Huang et al. (2013) to a predator–prey model with toxin effect. Our model consists of four equations. The first and second equations describe the prey and the predator growth rates, respectively, where the birth and death rates are explicit functions of body burdens. Body burden, which is also referred to as tissue residue in McElroy et al. (2010), is a direct measurement of toxin concentrations in the tissue or organism rather than in the exposure media. The third and fourth equations are the balance equations for the body burden of the two species, which describes the accumulation, the dilution of toxin in the organism tissue, and the transfer of toxin from prey to predator.

This model is then connected to experimental data via model parameterization. In particular, we consider the toxic effects of methylmercury on rainbow trout (*Oncorhynchus mykiss*) and its prey (small fish or aquatic insects) and obtain an appropriate estimate for each model parameter. The results of model parameterization and model analysis are used to numerically solve the model, and analyze the effect of the methylmercury on the end behavior of rainbow trout and its prey (small fish or aquatic insects). To qualitatively investigate the model, we simplify it to a two-dimensional system via a quasi-steady state approximation. We analyze the quasi-steady system by studying the effect of toxin level in the environment on existence and stability of steady states.

If there is no toxin, our toxin-dependent predator–prey model reduces to a classical predator–prey model, whose dynamics have been well studied. Thus, the main objective of this study is to investigate how the balance of the classical predator–prey dynamics will change when the toxin level in the environment varies from zero to higher levels. From our analysis and numerical exploration of the food web toxin model we found that toxin concentrations affect organisms at different trophic levels in a variety of ways. For example, high toxin concentrations in the environment are harmful to both species, and may lead to extirpation of both species. However, low toxin concentrations produce counterintuitive results. That is, contaminant effects on predators can actually lead to increased abundance of the prey.

The existence of limit cycles, where both population levels fluctuate around a coexistence equilibrium, is found in most classical predator–prey models. Our findings show that increasing toxin level may reduce and prevent populations from fluctuating when the predator and the prey are exposed simultaneously to a toxin.

Unlike most standard predator–prey systems, where populations will eventually tend towards only one stable steady state, our findings indicate that with a toxic effect, predator–prey systems may lead to multiple possible long-term outcomes. In this scenario, the initial population level will determine the final fate.

The rest of this paper is organized as follows. In Section 2, we develop a toxin-dependent predator–prey model. In Section 3, we connect the model to experiment data via model parameterization. We apply the results of model parameterization to consider the toxic effects of mercury on rainbow trout and its prey (small fish and aquatic insects). In Section 4, we reduce the dimensionality of the model using a quasi-steady state approximation. We then analyze the existence and stability of extinction and coexistence equilibria based on the quasi-steady system. In Section 5, we show possible asymptotic dynamics of the model. In Section 6, we study how toxin level in the environment affects the long-term behavior of the populations. Finally, a brief “Discussion” section completes the paper.

2. Model formulation

Since we are interested in an aquatic environment, we formulate the model in terms of concentration of population biomass, concentration of toxin in the population, and concentration of

toxin in the environment. In this study, we let

Concentration of population biomass
$$= \frac{\text{total mass of all individuals in the population}}{\text{volume of the total aquatic environment where the population lives}},$$

Concentration of toxin in the population
$$= \frac{\text{total mass of toxin contained in the population}}{\text{volume of the total aquatic environment}},$$

Concentration of toxin in the environment
$$= \frac{\text{total mass of toxin in the environment}}{\text{volume of the total aquatic environment}},$$

and

Body burden of population
$$= \frac{\text{total mass of toxin contained in the population}}{\text{total mass of all individuals in the population}}.$$

The state variables of the model are $x=x(t)$, the concentration of prey biomass in g/L at time t; $y=y(t)$, the concentration of predator biomass in g/L at time t; $U=U(t)$, the concentration of toxin contained in the prey in μg/L at time t; $V=V(t)$; the concentration of toxin contained in the predator in μg/L at time t; $u=u(t)$, the body burden of the prey in μg/g at time t; $v=v(t)$, the body burden of the predator in μg/g at time t.

A mathematical model that describes the effect of toxin on the predator–prey system is given by

$$\begin{aligned}
\underbrace{\frac{dx}{dt}}_{\text{rate of change of the concentration of prey biomass}} &= \underbrace{b(u,x)x}_{\text{gain due to birth and growth}} - \underbrace{d_1(u)x}_{\text{loss due to death}} - \underbrace{p(x)y}_{\text{loss due to predation}},\\
\underbrace{\frac{dy}{dt}}_{\text{rate of change of the concentration of predator biomass}} &= \underbrace{e(v)p(x)y}_{\text{gain due to birth and growth}} - \underbrace{d_2(v)y}_{\text{loss due to death}},\\
\underbrace{\frac{dU}{dt}}_{\text{rate of change of the concentration of toxin in the prey}} &= \underbrace{a_1Tx}_{\text{uptake from environment}} - \underbrace{\sigma_1U}_{\text{depuration due to metabolism}} - \underbrace{d_1(u)U}_{\text{loss due to death}} - \underbrace{p(x)yu}_{\text{loss due to predation}},\\
\underbrace{\frac{dV}{dt}}_{\text{rate of change of the concentration of toxin in the predator}} &= \underbrace{a_2Ty}_{\text{uptake from environment}} - \underbrace{\sigma_2V}_{\text{depuration due to metabolism}} - \underbrace{d_2(v)V}_{\text{loss due to death}} + \underbrace{p(x)yu}_{\text{gain due to predation}},\\
\underbrace{u=U/x}_{\text{body burden of prey}}, &\qquad \underbrace{v=V/y}_{\text{body burden of predator}},
\end{aligned} \tag{1}$$

with appropriate initial conditions, which describe the initial concentrations of prey and predator biomass and toxin concentrations.

The first equation presents a generic description of the growth of prey under the influence of the toxin. The second equation describes the growth of predator under the influence of the toxin. The third and fourth equations are balance equations for the concentrations of the toxin contained in the individuals of prey and predator, respectively.

The function $b(u,x)$ represents the biomass gain rate of the prey due to reproduction and growth; $d_1(u)$ denotes the biomass loss rate of the prey due to death; $d_2(v)$ represents the biomass loss rate of the predator due to death; $p(x)$ is the predator functional response that specifies the rate at which prey is consumed, per predator, as a function of the prey density; $e(v)$ is the production efficiency. We will introduce specific expressions for the functions $b(u,x)$, $d_1(u)$, $d_2(v)$, $p(x)$, and $e(v)$ at the end of this section.

The toxin uptake rates by the population from the environment, a_1Tx and a_2Ty, are modeled according to the *Law of Mass Action* and are proportional to both the concentration of toxin in the environment, T, and the concentration of population biomass, In this model a_1 and a_2 are the uptake coefficients for the prey and the predator, respectively. The positive constants σ_1 and σ_2 are the toxin depuration rates of the prey and the predator, respectively due to the metabolic process. The death of an individual leads to not only a loss of population biomass, but also a loss of internal toxin concentration. This leads to the term $-d_1(u)x$ in the first equation and the term $-d_1(u)U$ in the third equation. The predation of prey by predator leads to both a loss of the prey biomass and a gain of the predator biomass; accordingly, it leads to a transfer of toxin from the prey to the predator. This results in the term $-p(x)yu$ in the third equation and the term $p(x)yu$ in the fourth equation.

From the first two equations of the model (1), we notice that the direct influences of toxin on the growth of populations are implemented through their body burdens u and v. This motivates us to write down the equations describing the rate of change of u and the rate of change of v. As we will see, this allows us to study an equivalent system involving four state variables and four equations, instead of the model (1) which includes six state variables and six equations.

From the fifth equation of (1), we have

$$\frac{du}{dt} = \frac{U'}{x} - \frac{U}{x}\frac{x'}{x}. \tag{2}$$

Substituting the first equation and the third equation of (1) into (2), we obtain

$$\begin{aligned}
\frac{du}{dt} &= a_1T - [\sigma_1 + d_1(u)]u - \frac{p(x)y}{x}u - \left[b(u,x) - d_1(u) - \frac{p(x)y}{x}\right]u\\
&= a_1T - \sigma_1u - b(u,x)u.
\end{aligned} \tag{3}$$

Similar calculations in terms of the last, second and fourth equations of (1) give

$$v' = \frac{V'}{y} - \frac{V}{y}\frac{y'}{y} = a_2T - \sigma_2v + p(x)[u - e(v)v]. \tag{4}$$

Combining the first two equations of (1) and Eqs. (3) and (4), we have

$$\begin{aligned}
\frac{dx}{dt} &= b(u,x)x - d_1(u)x - p(x)y,\\
\frac{dy}{dt} &= e(v)p(x)y - d_2(v)y,
\end{aligned}$$

$$\frac{du}{dt} = a_1 T - \sigma_1 u - b(u,x)u,$$
$$\frac{dv}{dt} = a_2 T - \sigma_2 v + p(x)[u - e(v)v]. \tag{5}$$

We now introduce specific forms for the functions $b(u,x)$, $d_1(u)$, $d_2(v)$, $p(x)$, and $e(v)$. Following Huang et al. (2013), we let

$$b(u,x) = \frac{\alpha_1 \max\{0, 1-\alpha_2 u\}}{1+\alpha_3 x}, \tag{6}$$

with positive constants α_i $(i=1,2,3)$. Here the term $\alpha_1/(1+\alpha_3 x)$, which is a decreasing function with respect to prey biomass, represents a density-dependent per unit biomass gain rate. The term $\max\{0, 1-\alpha_2 u\}$, which is a fraction between 0 and 1, represents a linear dose response for the gain rate. If there is no toxic effect (body burden $u=0$), then $\max\{0, 1-\alpha_2 u\} = 1$, hence the gain rate of prey biomass is given by $\alpha_1/(1+\alpha_3 x)$. If the body burden u reaches a threshold level $1/\alpha_2$, then the individuals in the prey stop reproduction and growth, hence the gain rate of prey biomass is 0. A derivation of the expression (6) from a resource–consumer model via a time scale argument is presented in Thieme (2003).

For convenience, many researchers rewrite the above Type II functional response as

$$p(x) = \frac{\xi x}{\eta + x}, \tag{9}$$

where $\xi = 1/h$ and $\eta = 1/(\gamma h)$ (Kot, 2001). Since $p(\eta) = \xi/2$, η is referred as the half-saturation constant. In this study, we choose (9) as the expression of the functional response.

We assume that the dependence of the reproduction efficiency of the predator on its body burden v is given by

$$e(v) = \beta_1 \max\{0, 1-\beta_2 v\}, \tag{10}$$

here $0 < \beta_1 < 1$. The term $\max\{0, 1-\beta_2 v\}$ represents a linear dose response for the reproduction efficiency. If there is no toxic effect (body burden $v=0$), then $\max\{0, 1-\alpha_2 u\} = 1$, hence the reproduction efficiency is β_1. If the body burden v reaches a threshold level $1/\beta_2$, the reproduction efficiency is 0, which means that predators stop reproduction and growth.

Therefore, in this study we propose the following toxin-dependent predator–prey system

$$\begin{aligned}
\underbrace{\frac{dx}{dt}}_{\substack{\text{rate of change of the}\\ \text{concentration of prey biomass}}} &= \underbrace{\frac{\alpha_1 \max\{0,1-\alpha_2 u\}x}{1+\alpha_3 x}}_{\substack{\text{gain due to}\\ \text{birth and growth}}} - \underbrace{(k_1 u + m_1)x}_{\substack{\text{loss due}\\ \text{to death}}} - \underbrace{\frac{\xi x y}{\eta + x}}_{\substack{\text{loss due}\\ \text{to predation}}},\\
\underbrace{\frac{dy}{dt}}_{\substack{\text{rate of change of the}\\ \text{concentration of predator biomass}}} &= \underbrace{\frac{\beta_1 \xi x y \max\{0,1-\beta_2 v\}}{\eta + x}}_{\substack{\text{gain due to}\\ \text{birth and growth}}} - \underbrace{(k_2 v + m_2)y}_{\substack{\text{loss due}\\ \text{to death}}},\\
\underbrace{\frac{du}{dt}}_{\substack{\text{rate of change of the}\\ \text{body burden of the prey}}} &= \underbrace{a_1 T}_{\substack{\text{uptake from}\\ \text{environment}}} - \underbrace{\sigma_1 u}_{\substack{\text{depuration due}\\ \text{to metabolism}}} - \underbrace{\frac{\alpha_1 \max\{0,1-\alpha_2 u\}}{1+\alpha_3 x} u}_{\substack{\text{dilution due to}\\ \text{birth and growth}}},\\
\underbrace{\frac{dv}{dt}}_{\substack{\text{rate of change of the}\\ \text{body burden of the predator}}} &= \underbrace{a_2 T}_{\substack{\text{uptake from}\\ \text{environment}}} - \underbrace{\sigma_2 v}_{\substack{\text{depuration due}\\ \text{to metabolism}}} + \underbrace{\frac{\xi x}{\eta + x} u}_{\substack{\text{gain due}\\ \text{to predation}}}\\
&\quad - \underbrace{\frac{\xi x}{\eta + x} \beta_1 \max\{0, 1-\beta_2 v\} v}_{\substack{\text{dilution due to}\\ \text{birth and growth}}}.
\end{aligned} \tag{11}$$

In 1992, the committee on toxicology of the National Research Council recommended the use of the power law to study the relationship between toxin concentration and mortality rate since it has been shown to fit the data well (Miller and Janszen, 2000). Here, for model analysis, we assume a special case of power law with power one. That is, we assume that mortality rates $d_1(u)$ and $d_2(v)$ linearly depend on their body burdens u and v, respectively. Thus, taking natural mortality rates into account, we let

$$d_1(u) = k_1 u + m_1, \quad d_2(v) = k_2 v + m_2, \tag{7}$$

where k_1, m_1, k_2, m_2 are positive constants.

The predator functional response describes a predator's per capital feeding rate. Here we use a Type II functional response (Holling, 1959) which is more realistic than Type I (e.g., Polis et al., 1989) as it incorporates predator satiation through the assumption that predators have a prey handling time. In this case, the per capita feeding rate of the predator is given by a function of the form

$$p(x) = \frac{\gamma x}{1 + \gamma h x}, \tag{8}$$

where γ is the encounter rate (or capture efficiency) and h is the handling time.

In the absence of predator, the model (11) reduces to the one species toxin-dependent model studied in Huang et al. (2013).

3. Parameterization and numerical results

While our toxin-dependent predator–prey model (11) is general, we apply it to consider the effect of a toxin on the dynamics of fish and its prey. In this section, we first describe the parameterization of the model (11) by choosing rainbow trout as our representative predatory fish and small fish or aquatic insects as the prey. The results of model parameterization are then used to illustrate the impact of methylmercury on the long-time behavior of rainbow trout and its prey (small fish or aquatic insects).

Rainbow trout are found widely throughout the world. However some populations such as the native rainbow trout population in the Athabasca River, Alberta, and rainbow trout found in watersheds west of the Cascade Mountains in the U.S. are threatened. Rainbow trout routinely feed on larval, pupal and adult forms of aquatic insects (typically caddisflies, stoneflies, mayflies and aquatic diptera), and small fish up to one-third of their length.

The toxic effects of methylmercury exposure in fish and wildlife species are well documented (reviewed by Sandheinrich and

Wiener, 2011). The United States Geological Survey developed the National Descriptive Model for Mercury in Fish (Wente, 2004) to partition variation in methylmercury concentration due to size, species and sample type across space and time. The Canadian Fish Mercury Database includes over 330,000 records representing 104 species of freshwater fish collected from over 5000 locations across Canada between 1967 and 2010 (Depew et al., 2013). Mercury may be released into the aquatic environment in states of relatively low toxicity, but will be transformed into highly toxic states, namely methylmercury. Mercury's harmful effects on fish include death, reduced reproduction, slower growth and development, and abnormal behavior (Eisler, 1987). Methylmercury is of special concern, not only because of its toxicity, but also because of its tendency to biomagnify in upper trophic levels of aquatic food webs (Canadian Council of Ministers of the Environment, 2003b).

As we mentioned earlier, in the absence of the predator, the toxin-dependent predator–prey system (11) reduces to a one species toxin-dependent model which we developed in Huang et al. (2013). Therein, we considered the toxic effect of methylmercury on rainbow trout (*Oncorhynchus mykiss*) and obtained an appropriate range for each model parameter. To make parameterization for the model (11), we first apply the results of parameter estimate in Huang et al. (2013) to those predator-related parameters in the model (11). We then connect the model to experiment data to estimate the prey (aquatic insects)-related parameters.

3.1. Predator (rainbow trout)-related parameters

The parameter estimate results in Huang et al. (2013) are given by certain ranges (intervals), and here we take the midpoint of intervals as the corresponding parameter values and obtain the following: $\beta_2 = 33.41$ in g/μg, $k_2 = 0.00398$ in g/μg/day, $m_2 = 0.00057$ in day^{-1}, $a_2 = 0.1733$ in day^{-1}, and $\sigma_2 = 0.0062$ in day^{-1}.

The carrying capacity of rainbow trout was estimated as $\eta = 0.00091$ in g/L, hence we take the half-saturation constant $\eta = 0.000455$ in g/L.

The maximum growth rate of rainbow trout is estimated as 0.0047 in day^{-1}. This corresponds to the term $\frac{\beta_1 \xi x}{\eta + x}$ in (11). For simplicity, letting $\frac{\beta_1 \xi x}{\eta + x} = 0.0047$ and $x \to \infty$, we get $\beta_1 \xi = 0.0047$ in day^{-1}. It is commonly assumed that transfer efficiency between trophic level is 0.1 (Bax, 1998). Letting $\beta_1 = 0.1$, we obtain $\xi = 0.047$ in day^{-1}.

3.2. Prey (aquatic insects)-related parameters

It is difficult to find experimental results for one species of aquatic insects to estimate all model parameters. In what follows, we choose data for several related species to roughly estimate the prey related parameters in the model (11).

3.2.1. Maximum reproduction rate α_1 and natural mortality rate m_1

We choose caddisflies to estimate maximum reproduction rate α_1 and the natural mortality rate m_1 for the prey. The caddisflies are an order, Trichoptera, of insects with approximately 12,000 described species. Caddisflies in most temperate areas complete their life cycles in a single year, from egg to larva, to pupa, then adult; most caddisfly larvae (caddis worms) live about one year in the aquatic environment before pupating; The adult stage of caddisflies, in most cases, is very short-lived, usually only 1–2 weeks. Caddisfly adults live just long enough to mate, they do not eat and focus only on reproduction. Each adult female can lay up to 800 eggs (Hildrew and Rüdiger, 1992). Willis and Hendricks (1992) studied the life history and production of hydropsychid caddisflies in Mill Creek, Virginia. They found that only about 0.5% of the original eggs survived to adulthood. This finding is in close agreement with the findings of Elliott (1981, 1982) that survival to reproduction in *Philopotamus montanus* was 0.4% and survival from egg to imago in *Potamophylax cingulatus* was 1–2%. By assuming 1:1 female–male ratio we choose the maximum reproduction rate of caddisflies $\alpha_1 = 800 \times 0.5 \times 1\%/365 = 4/365$ in day^{-1}.

We take the natural mortality rate $m_1 = 1/365$ in day^{-1} by assuming that the average natural life span of caddisfly is 365 days.

3.2.2. Crowding effect α_3

We estimate the crowding effect parameter α_3 by using the estimated carrying capacity of aquatic insect populations in the literature (Gilpin and Ayala, 1973). The carrying capacities of two species of Drosophila were estimated by fitting two analytic models to experimental data. The mean of the carrying capacities of two species, denoted by K, is 0.0011 g/L. We use the carrying capacity, K, to the crowding effect parameter α_3 as follows.

If there is no toxin or predation, the first equation of (11) becomes

$$\frac{dx}{dt} = \left(\frac{\alpha_1}{1+\alpha_3 x} - m_1\right)x = \frac{(\alpha_1 - m_1)\left(1 - \frac{x}{K}\right)x}{1+\alpha_3 x}, \tag{12}$$

with

$$K = \frac{\alpha_1 - m_1}{m_1 \alpha_3}. \tag{13}$$

Notice that $\alpha_1 - m_1$ is always positive from the estimated values for α_1 and m_1. It is not difficult to check that K plays the role of the carrying capacity as with the logistic equation. Using the above equation and taking the estimates of α_1 and m_1 into accounting, we obtain $\alpha_3 = 1330$ in L/g.

3.2.3. Uptake rate a_1 and depuration rate σ_1

Next we estimate the toxin-related parameters in the model (11) for aquatic insects. The uptake rate constants and depuration rates for mercury by four aquatic insect species (two caddisflies and two mayflies) were estimated by Xie et al. (2009). We choose uptake coefficient of the prey (aquatic insects) to be the mean of the four uptake rate constants and obtain the estimate: $a_1 = 0.55$ in L/g/day. We choose depuration rate of aquatic insects to be the mean of the four depuration rates and obtain the estimate: $\sigma_1 = 0.12$ in day^{-1}.

3.2.4. Effect of toxin on reproduction α_2

Abnoos et al. (2013) studied the effect of mercury on the development of stage of eggs to adult fruit fly (*Drosophis melanogaster*). They showed that the maturity percentage and percentage of hatched eggs of the fruit fly are approximately 100% in 10 μg/L of methyl mercury (Table 1 in Abnoos et al., 2013). We use this data to estimate the parameter α_2 that describes the effect of toxin on reproduction of the prey. From the third equation of system (11), the relationship between the concentration of mercury in the environment T and the body burden of fruit fly u is approximately given by

$$u = \frac{a_1}{\sigma_1} T. \tag{14}$$

(This quasi-steady state approximation will be discussed in Section 4.2.) We choose the threshold body burden $\frac{1}{\alpha_2} = \frac{a_1}{\sigma_1} T$, at which fruit fly stop reproduction. Using the above estimates of a_1 and σ_1 and letting $T = 10$ μg/L, we estimate $\alpha_2 = 0.022$ in g/μg. This estimate implies that fruit fly is much less sensitive to mercury than rainbow trout since α_2 is much less that β_2 (equal to 33.41 g/μg) that describes the effect of methylmercury on the reproduction of rainbow trout.

3.2.5. Coefficient of mortality rate k_1

The lethal and sublethal responses of an aquatic insect, the southern house mosquito (*Culex quinquefasciatus: Diptera*), to a range of methyl mercury concentrations were studied by Jensen et al. (2007). The percent mortalities of *Culex quinquefasciatus* are 28.5%, 29%, 44.5%, and 93%, respectively when exposed to 1.5 μg/L, 3 μg/L, 7.5 μg/L and 15 μg/L methylmercury, for 11 days (Table 1 in Jensen et al., 2007).

The relationship between the percent mortality after t days, denoted by $p_0(t)$, and the toxin related mortality rate k_1u was described by

$$p_0(t) = 1 - \exp\{-k_1 ut\} \tag{15}$$

in Huang et al. (2013). Substituting (14) into (15) and letting $t=11$ in day, $a_1=0.55$ in L/g/day, $\sigma_1 = 0.12$ in day^{-1} (estimated in Section 3.2.3), we have

$$p_0(t) = 1 - \exp\left\{-k_1 \frac{a_1 Tt}{\sigma_1}\right\}. \tag{16}$$

Using the mortality rate function (16) and employing Matlab routine LSQCURVEFIT to fit the above-mentioned data (Table 1 in Jensen et al., 2007), we obtain parameter estimate $k_1=0.0021$ in g/μg/day.

We list rainbow trout- and aquatic insect-related parameter estimates in Table 1.

3.3. Numerical results

In what follows, we use the parameter estimates from Sections 3.1 and 3.2 to numerically solve the toxin-dependent predator–prey model (11). Our purpose is to understand how the concentration of methylmercury in the environment affects the long-term biomass of rainbow trout and its prey. We make numerical simulations by considering two predator–prey scenarios.

In the first scenario, we regard the rainbow trout as the predator and small fish as the prey. We assume that the small fish have the same vital rates and same sensitivity to methylmercury as the rainbow trout, and directly apply the results of model parameterization in Huang et al. (2013) to those prey-related parameters in the model (11). We plot the stable biomass of the prey (small fish) and the predator (rainbow trout) as the concentration of methylmercury increases from 0 to 0.0025 μg/L in Fig. 1.

In the second scenario, we regard the rainbow trout as the predator and aquatic insects as the prey. We apply the results of model parameterization from Sections 3.1 and 3.2 to the model (11). We plot the stable biomass of the prey (aquatic insects) and the predator (rainbow trout) as the concentration of methylmercury in the environment changes from 0 to 0.01 g/L in Fig. 2.

Fig. 1 shows that the stable predator (rainbow trout) biomass decreases as the concentration of methylmercury in the environment T changes from 0 to higher levels, which implies that the toxin is always harmful to the predator. However, as T increase but still at low levels, stable prey biomass increases, which indicates that low toxin concentrations benefit the prey (small fish). This is because toxic effects on the predator reduce its prey from predation. It can be observed that the threshold value of T for the rainbow trout extirpation is around 0.0020 μg/L even though the stable population level becomes very low as T reaches around 0.0005 μg/L. This result can be compared to that in our earlier work (Huang et al., 2013) based on a single-species model. Therein, we showed that the rainbow trout biomass decreases from a low level until it becomes extirpated when T increases from 0.0011 to 0.0045 μg/L (Fig. 3 in Huang et al., 2013). This is because unlike the previous single-species model in which rainbow trout was assumed to take up toxin only from water hence bioaccumulation (toxin uptake via food ingestion) was ignored, the toxin-related predator–prey model (11) considers two routes of toxin uptake by the predator. That is, rainbow trout uptake the toxin from both water and their food (small fish). The bioaccumulation in the higher-trophic level population (predator) leads to a higher body burden, which results in a lower threshold value of toxin in the environment for the predator extirpation.

Fig. 2 illustrates that the stable predator biomass decreases as the concentration of methylmercury increases, which leads to the stable aquatic insects biomass increasing until it reaches its environmental carrying capacity. This is because aquatic insects are much less sensitive to methylmercury than rainbow trout (see Section 3.2.4), when the toxin level in the environment is sufficiently high such that rainbow trout become extirpated, its prey (aquatic insects) is still be able to grow. Fig. 2 also shows that the threshold value of T for the

Table 1
Rainbow trout- and aquatic insect-related parameters.

Symbols	Definitions	Estimate values
α_1	Maximum reproduction rate of aquatic insects	4/365 day^{-1}
α_2	Effect of toxin on the growth of aquatic insects	0.022 g/μg
α_3	Crowding effect of aquatic insects	1330 L/g
k_1	Effect of toxin on the mortality of aquatic insects	0.0021 g/μg/day
m_1	Natural mortality rate of aquatic insects	1/365 day^{-1}
ξ	Per capita feeding rate	0.047 day^{-1}
η	Half-saturation constant	0.000455 g/L
β_1	Reproduction efficiency of rainbow trout	0.1
β_2	Effect of toxin on the reproduction of rainbow trout	33.41 g/μg
k_2	Effect of toxin on the mortality of rainbow trout	0.00398 g/μg/day
m_2	Natural mortality rate of rainbow trout	0.00057 day^{-1}
a_1	Uptake coefficient for aquatic insects	0.55 L/g/day
σ_1	Depuration rate for aquatic insects	0.12 day^{-1}
a_2	Uptake coefficient for rainbow trout	0.1733 L/g/day
σ_2	Depuration rate for rainbow trout	0.0062 day^{-1}

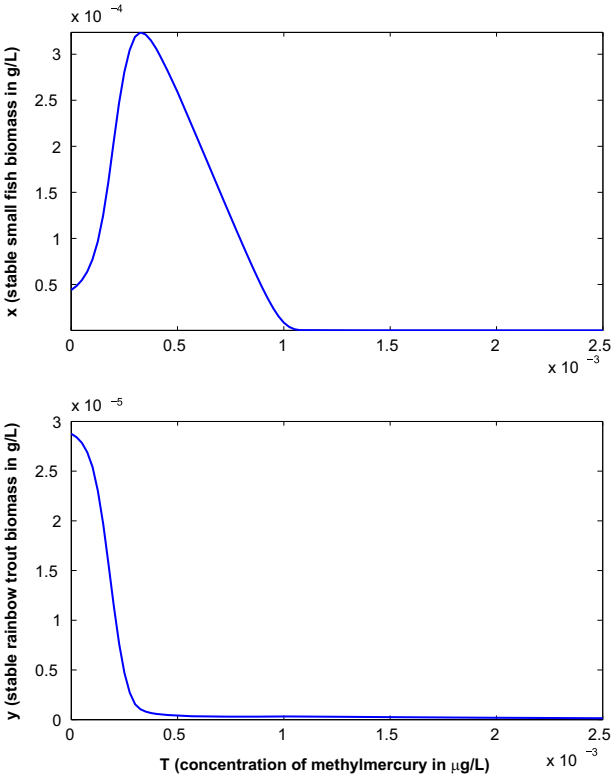

Fig. 1. The stable biomass of the prey (small fish) and the predator (rainbow trout) when the concentration of methylmercury in the environment changes from 0 to 0.0025 μg/L.

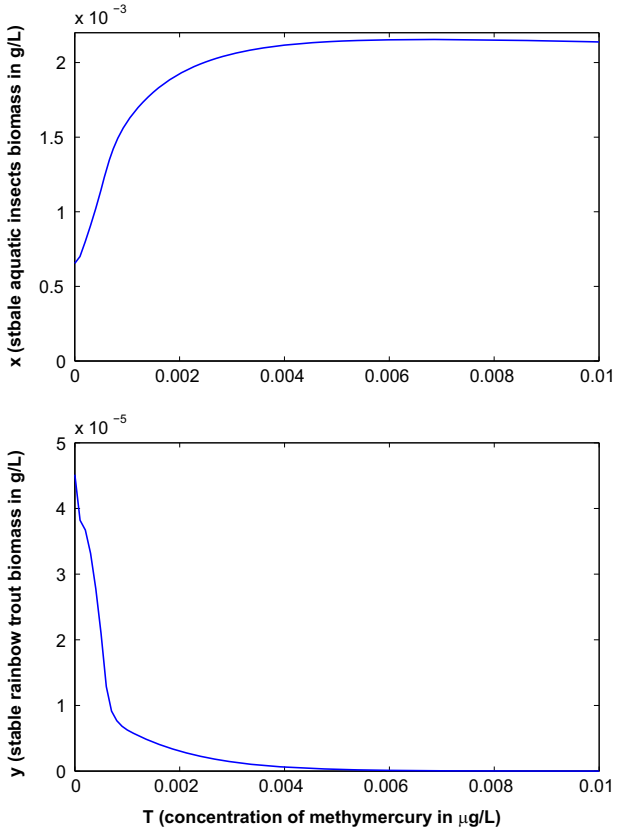

Fig. 2. The stable biomass of the prey (aquatic insects) and the predator (rainbow trout) when the concentration of methylmercury in the environment changes from 0 to 0.01 μg/L.

rainbow trout extirpation is around 0.006 μg/L, which is higher than that shown by Fig. 1. The reason for this is because the high prey density (aquatic insects) provides abundant food for the predator (rainbow trout) such that the predator is still able to survive in a environment with relatively high toxin concentrations.

4. Model analysis

We expect that the dynamics for the depuration due to metabolism of toxin will operate on a much faster time scale than the dynamics of population biomass growth. This means that the body burden equations may approach a quasi-equilibrium state where uptake of toxin and depuration balance out on a fast time scale. To investigate this process mathematically we define $\epsilon=\alpha_1/\sigma_1$ to be a small parameter. For example, we find that $\epsilon=0.091$ from the parameter estimates for aquatic insects and rainbow trout (See Table 1).

4.1. Nondimensionalization and nonnegativity

To simplify the problem and facilitate analysis, we rescale the system (11) by introducing the nondimensional quantities:

$$\tilde{x}=\alpha_3 x,\quad \tilde{y}=\frac{\alpha_3\xi}{\alpha_1}y,\quad \tilde{u}=\alpha_2 u,\quad \tilde{v}=\beta_2 v,\quad \tilde{t}=\alpha_1 t,$$
$$\tilde{k}_1=\frac{k_1}{\alpha_1\alpha_2},\quad \tilde{m}_1=\frac{m_1}{\alpha_1},\quad \tilde{\eta}=\alpha_3\eta,$$
$$\tilde{\beta}_1=\frac{\beta_1\xi}{\alpha_1},\quad \tilde{k}_2=\frac{k_2}{\alpha_1\beta_2},\quad \tilde{m}_2=\frac{m_2}{\alpha_1},$$
$$\tilde{T}=\frac{\alpha_2 a_1 T}{\sigma_1},\quad c=\frac{a_2\beta_2}{a_1\alpha_2},\quad \tilde{\sigma}_2=\frac{\sigma_2}{\sigma_1},\quad \tilde{\beta}_2=\frac{\beta_2\xi}{\alpha_2\sigma_1},\quad \epsilon=\frac{\alpha_1}{\sigma_1}. \tag{17}$$

Dropping the tildes for notational simplicity, we rewrite the system (11) in its dimensionless form:

$$\begin{aligned}
\frac{dx}{dt}&=\left(\frac{\max\{0,1-u\}}{1+x}-k_1u-m_1\right)x-\frac{xy}{\eta+x},\\
\frac{dy}{dt}&=\frac{\beta_1 xy\,\max\{0,1-v\}}{\eta+x}-(k_2v+m_2)y,\\
\epsilon\frac{du}{dt}&=T-u-\epsilon\frac{\max\{0,1-u\}}{1+x}u,\\
\epsilon\frac{dv}{dt}&=cT-\sigma_2 v+(\beta_2 u-\epsilon\beta_1\,\max\{0,1-v\}v)\frac{x}{\eta+x}.
\end{aligned} \tag{18}$$

We first show that solutions of system (18) behave in a biologically reasonable manner. That is, the population densities at any time, which are given by the solutions of the model at time t, are always nonnegative but not arbitrarily large.

Theorem 4.1. *Each component of the solution of system (18) with nonnegative initial conditions remains bounded and nonnegative for all $t>0$.*

See Appendix A for the proof.

4.2. Quasi-steady system

Because the model (18) is a high dimensional system, the stability analysis of model (18) is challenging. We simplify it to a two-dimensional system via the quasi-steady state approximation. Since ϵ is introduced as a small parameter, letting $\epsilon\to 0$ in (18), we have

$$u=T,\quad v=\frac{cT}{\sigma_2}+\frac{\beta_2 T}{\sigma_2}\frac{x}{\eta+x}. \tag{19}$$

Substituting (19) into the first and second equations of (18), we obtain the following quasi-steady system:

$$\begin{aligned}
\frac{dx}{dt}&=\left(\frac{\max\{0,1-T\}}{1+x}-k_1T-m_1\right)x-\frac{xy}{\eta+x},\\
\frac{dy}{dt}&=\frac{\beta_1 xy\,\max\left\{0,1-\frac{cT}{\sigma_2}-\frac{\beta_2 T}{\sigma_2}\frac{x}{\eta+x}\right\}}{\eta+x}\\
&\quad-\left[k_2\left(\frac{cT}{\sigma_2}+\frac{\beta_2 T}{\sigma_2}\frac{x}{\eta+x}\right)+m_2\right]y.
\end{aligned} \tag{20}$$

Throughout this paper, we assume that

$$m_1<1\quad\text{and}\quad T<\min\{1,\sigma_2/c\}. \tag{21}$$

These mean that the natural loss rate of the prey biomass due to death is less than its maximum gain rate due to birth and growth, and that the environmental toxin levels are low enough that the prey can reproduce and grow. If either of these conditions is violated then the prey cannot persist and both prey and predator are extirpated (see Appendix B for further discussion).

We also assume that

$$m_2<\beta_1. \tag{22}$$

This means that the natural loss rate of the predator biomass due to death is less than its maximum gain rate due to birth and growth. If this condition is violated then the predator is extirpated, the system (20) reduces to a one species model (see Appendix B).

With these assumptions, the nondimensionalized system (20) can be rewritten as

$$\begin{aligned}
\frac{dx}{dt}&=f(x)-\varphi(x)y,\\
\frac{dy}{dt}&=g(x)y,
\end{aligned} \tag{23}$$

with

$$f(x)=\left(\frac{1-T}{1+x}-k_1T-m_1\right)x, \tag{24}$$

$$\varphi(x)=\frac{x}{\eta+x}, \tag{25}$$

and

$$g(x)=\beta_1\varphi(x)\max\left\{0,1-\frac{cT}{\sigma_2}-\frac{\beta_2T}{\sigma_2}\varphi(x)\right\}-\frac{k_2cT}{\sigma_2}-\frac{k_2\beta_2T}{\sigma_2}\varphi(x)-m_2. \tag{26}$$

4.2.1. Existence of equilibria

To investigate the long-term behavior of the system (23), we look for the steady states (equilibria) where either one or both species survive. These can be found by finding the intersections of prey and predator zero-growth isoclines (or null-clines), where either prey or predator growth rate is zero. We summarize the existence of extirpation and coexistence equilibria and corresponding conditions required in Table 2. The detailed discussion is provided in Appendix C.

In Table 2,

$$T_0^*=\frac{1-m_1}{k_1+1},$$

$$T_1^*:=\frac{\beta_1\sigma_2(\beta_1c+k_2\beta_2+2\beta_2m_2)-\beta_1\sigma_2\sqrt{4\beta_2(\beta_1c+\beta_2m_2)(m_2+k_2)}}{(\beta_1c-k_2\beta_2)^2},$$

$$T_2^*=\frac{(\beta_1-m_2)\sigma_2}{\beta_1\beta_2+\beta_1c+k_2\beta_2+k_2c},$$

$$T_3^*=\frac{\beta_1\sigma_2}{\beta_1c+k_2\beta_2+2\beta_1\beta_2},$$

$$x_0=(1-T)/(k_1T+m_1)-1,$$

$$x_{1,2}=\frac{\eta\varphi_{1,2}}{1-\varphi_{1,2}},$$

$$\varphi_{1,2}=\frac{\beta_1(\sigma_2-cT)-k_2\beta_2T\mp\sqrt{\Delta}}{2\beta_1\beta_2T},$$

$$\Delta=[\beta_1(\sigma_2-cT)-k_2\beta_2T]^2-4\beta_1\beta_2T(k_2cT+m_2\sigma_2).$$

As shown in Table 2, the conditions of the existence of equilibria are given by the restriction conditions with respect to the toxin level in the environment T and the half-saturation constant η that is related to the capture efficiency. Note that the quantities $T_0^*, T_1^*, T_2^*, T_3^*$ are independent of T and η, if we assume that these quantities are constant, then the magnitudes of toxin concentration in the environment and the half-saturation constant determine the number of equilibria.

It is worth mentioning that in row C of Table 2, the condition $T<\min\{T_0^*,T_1^*,T_2^*\}$ guarantees that $x_0>0$ and $\varphi_1<1$, hence $x_0/\varphi_1-x_0>0$ and the condition $\eta<x_0/\varphi_1-x_0$ plays a role.

Row D of Table 2 implies that very strict conditions are required to guarantee the existence of another coexistence equilibrium E_2. The first condition $\max\{T_2^*,T_3^*\}<\min\{T_0^*,T_1^*\}$ allows for the possibility that the toxin level lies within the range $(\max\{T_2^*,T_3^*\}<T<\min\{T_0^*,T_1^*\})$. The condition $T<\min\{T_0^*,T_1^*\}$ guarantees that $x_0>0$ and $\varphi_2>0$. The condition $T>\max\{T_2^*,T_3^*\}$ guarantees that $\varphi_2<1$. Thus, $x_0/\varphi_2-x_0>0$ and it is possible that the last condition $\eta<x_0/\varphi_2-x_0$ can be realized.

Recall that the half saturation constant $\eta=1/(\gamma h)$ (see Eqs. (8) and (9)), where γ is the encounter rate (or capture efficiency) and h is the handling time. If we assume that the handling time h is constant, then a small half-saturation constant means that a high capture efficiency and a large half-saturation constant correspond to a low capture efficiency. Thus, the conditions $\eta<x_0/\varphi_1-x_0$ and $\eta<x_0/\varphi_2-x_0$ in Table 2 can be interpreted as the predator requiring sufficiently high capture efficiencies.

Fig. 3 illustrates several possible null-clines where either the prey or the predator growth rate is zero. At the intersections of the prey and predator null-clines, we find equilibrium points. In all panels of Fig. 3, the conditions $\max\{T_2^*,T_3^*\}<\min\{T_0^*,T_1^*\}$ and $\max\{T_2^*,T_3^*\}<T<\min\{T_0^*,T_1^*\}$ are satisfied, hence the boundary equilibria $E_{0,1}$ and $E_{0,2}$ always exist.

As shown in Fig. 3, depending on the values of η which determines the intersections of the null-clines, the system may have zero, one or two coexistence equilibria. In the left panel, $\eta>x_0/\varphi_1-x_0$, the system has no coexistence equilibrium. In the middle panel, $x_0/\varphi_2-x_0<\eta<x_0/\varphi_1-x_0$, the system has only one coexistence equilibrium E_1. In the right panel, $\eta<x_0/\varphi_2-x_0$, the system has two coexistence equilibria E_1 and E_2.

4.2.2. Stability of equilibria

To analyze the stability of an equilibrium, we may use the Jacobian matrix if the eigenvalues of the Jacobian evaluated at the equilibrium have nonzero real parts. The Jacobian matrix for system (23) is

$$J=\begin{pmatrix} f'(x)-\varphi'(x)y & -\varphi(x) \\ g'(x)y & g(x)\end{pmatrix} \tag{27}$$

To assess the stability of extirpation equilibrium $E_{0,2}$, we need another quantity measuring the external toxin level, that is,

$$T_4^*:=\frac{\beta_1\sigma_2(\beta_1c+k_2\beta_2+2\beta_2m_2)+\beta_1\sigma_2\sqrt{4\beta_2(\beta_1c+\beta_2m_2)(m_2+k_2)}}{(\beta_1c-k_2\beta_2)^2}. \tag{28}$$

We make the following conclusions regarding the stability of extirpation equilibria. The proof is provided in Appendix D.

Table 2
The existence of equilibria.

	Mathematical conditions	Equilibria	Biological interpretations
A	$T>T_0^*$	$E_{0,1}=(0,0)$	System only has extinction equilibrium if external toxin level is high enough that neither population persists
B	$T<T_0^*$	$E_{0,1}$ and $E_{0,2}=(x_0,0)$	System has extinction and prey-only equilibria if toxin level is low enough that prey can survival but predator cannot
C	$\max\{T_2^*,T_3^*\}>\min\{T_0^*,T_1^*\}$ $T<\min\{T_0^*,T_1^*,T_2^*\}$ $\eta<\frac{x_0}{\varphi_1}-x_0$	$E_{0,1}$, $E_{0,2}$, and $E_1=\left(x_1,\frac{f(x_1)}{\varphi(x_1)}\right)$	A coexistence equilibrium appears if toxin level and the half-saturation constant are sufficiently low such that both populations can coexist
D	$\max\{T_2^*,T_3^*\}<\min\{T_0^*,T_1^*\}$ $\max\{T_2^*,T_3^*\}<T<\min\{T_0^*,T_1^*\}$ $\eta<\frac{x_0}{\varphi_2}-x_0$	$E_{0,1}$, $E_{0,2}$, E_1, and $E_2=\left(x_2,\frac{f(x_2)}{\varphi(x_2)}\right)$	System has two coexistence equilibria when toxin level lies on a certain range and the half-saturation constant is sufficiently low such that both populations can coexist

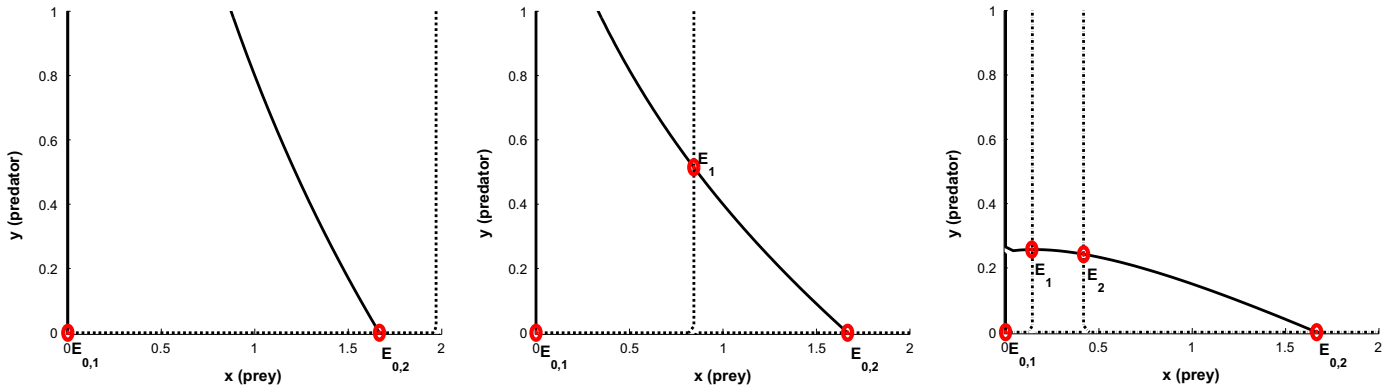

Fig. 3. Possible null-clines for system (22) with the parameter values, $T=0.2$, $k_1=1$, $m_1=0.1$, $\beta_1=1$, $\beta_2=4$, $c=1.5$, $\sigma_2=1$, $k_2=0.2$, $m_2=0.02$, and different values of η: (left) $\eta=7$, (middle) $\eta=3$, (right) $\eta=0.5$. Solid curves are the prey null-clines and dashed lines are the predator null-clines. Circles indicate equilibrium points.

Theorem 4.2. *(1) The extirpation equilibrium $E_{0,1}=(0,0)$ is globally asymptotically stable if $T>(1-m_1)/(k_1+1)$. $E_{0,1}$ is an unstable saddle point if $T<(1-m_1)/(k_1+1)$.*

(2) The prey-only equilibrium $E_{0,2}=(x_0,0)$ is locally asymptotically stable if one of the following conditions is satisfied: (i) $T_1^*<T<T_4^*$, (ii) $T<T_1^*$ *and* $\eta>x_0/\varphi_1-x_0$, *and* (iii) $\max\{T_2^*,T_3^*\}<\min\{T_0^*,T_1^*\}$, $\max\{T_2^*,T_3^*\}<T<\min\{T_0^*,T_1^*\}$, *and* $\eta<\frac{x_0}{\varphi_2}-x_0$.

The mathematical results in Theorem 4.2 can be interpreted as follows:

(1) If the external toxin level is sufficiently high ($T>(1-m_1)/(k_1+1)$), then from Table 2, we see that the extirpation equilibrium $E_{0,1}=(0,0)$ is the only stable state of the system. Hence the solutions of the system must tend towards this equilibrium, which means that both populations are extirpated.

(2) In the following scenarios, the prey can survive but the predator cannot:
   (i) If the external toxin level falls into a certain range ($T_1^*<T<T_4^*$), only the prey can persist because the toxin level is sufficiently low ($T<T_4^*$). However, it is too high ($T>T_1^*<T$) for the predator to persist.
   (ii) The toxin level is sufficiently low ($T<T_1^*$) such that the prey can persist. The predator is extirpated because the half-saturation constant is too large ($\eta>x_0/\varphi_1-x_0$) (i.e., the capture efficiency is too low), which leads to a low growth rate of the predator.

For coexistence equilibria, we have the following results. The proof is provided in Appendix E.

Theorem 4.3. *The equilibrium E_1 is locally asymptotically stable if either $\eta\le 1$ or both conditions $0<\eta<1$ and $k_1T+m_1>\frac{(1-\eta)(1-T)}{(1+x_1)^2}$ are satisfied. The equilibrium E_2 is always an unstable saddle point.*

Combining the condition of existence (Table 2) and the condition of stability (Theorem 4.3) of the coexistence equilibrium E_1, we find that the both populations can coexist in the following two scenarios:

(1) Both populations coexist at the equilibrium E_1 if the half-saturation constants lie within a certain range ($1\le\eta<\frac{x_0}{\varphi_1}-x_0$) (i.e., the capture efficiency lies within a certain range) and the toxin-dependent mortality rate of the prey is sufficiently low ($k_1T+m_1<(1-T)(1-\varphi_1)$). This is because of the condition of the existence of E_1, $\eta<\frac{x_0}{\varphi_1}-x_0$, the condition $\eta\ge 1$ plays a role only when $\frac{x_0}{\varphi_1}-x_0>1$, which is equivalent to $k_1T+m_1<(1-T)(1-\varphi_1)$.

(2) Both species coexist at the equilibrium E_1 if the half-saturation constants are sufficiently small ($0<\eta<1$) (i.e., the capture efficiencies are sufficiently high) and the prey has an intermediate mortality rate ($\frac{(1-\eta)(1-T)}{(1+x_1)^2}<k_1T+m_1<\frac{1-T}{1+x_1}$).This is because we can equivalently rewrite the condition of the existence of E_1, $\eta<\frac{x_0}{\varphi_1}-x_0$, as $k_1T+m_1<\frac{1-T}{1+x_1}$. Thus, from Theorem 4.3, we see that both populations are able to coexist at E_1 if both conditions $0<\eta<1$ and $\frac{(1-\eta)(1-T)}{(1+x_1)^2}<k_1T+m_1<\frac{1-T}{1+x_1}$ are satisfied.

From the discussion in this section, we know that the quasi-steady system (20) has at most two boundary equilibria $E_{0,1}$ (both extirpation) and $E_{0,2}$ (only prey) and two interior (coexistence) equilibria E_1 and E_2 which depends on the intersections of the null-clines. We also show that the stability of these equilibria can be guaranteed if the toxin level T and half saturation constant η satisfy certain conditions.

5. Numerical observations of asymptotic dynamics

In this section, we show a variety of long-term asymptotic dynamics that the system (20) may exhibit based on the results of the existence and stability of equilibria. To do so, we plot phase portraits (Figs. 4–7) using the existing open MATLAB program pplane8.m by choosing different parameter values. The phase portraits illustrate different types of eventual behavior of the populations.

As we observe from Figs. 4 to 7, The asymptotic dynamics (i.e., the eventual behavior of the populations) can be grouped into six general structures: extirpation of both species (extirpation equilibrium $E_{0,1}$ is globally asymptotically stable); prey-only extirpation (extirpation equilibrium $E_{0,2}$ is globally asymptotically stable); coexistence at an interior equilibrium point (coexistence equilibrium $E_{0,2}$ is globally asymptotically stable); coexistence with periodical population oscillation which decreases in amplitude as T increases (system has a globally asymptotic stable limit cycle); bistability where both the extirpation equilibrium $E_{0,2}$ and the interior equilibrium point E_1 are locally asymptotic stable; bistability where system has a stable limit cycle and a stable prey-only equilibrium.

Fig. 4 shows several types of global stability. The top left panel of Fig. 4 shows that both species are extirpated when the toxin level in the environment T is high and leads to high population mortality rates and low population growth rates. The top right panel of Fig. 4 shows that the prey excludes the predator when

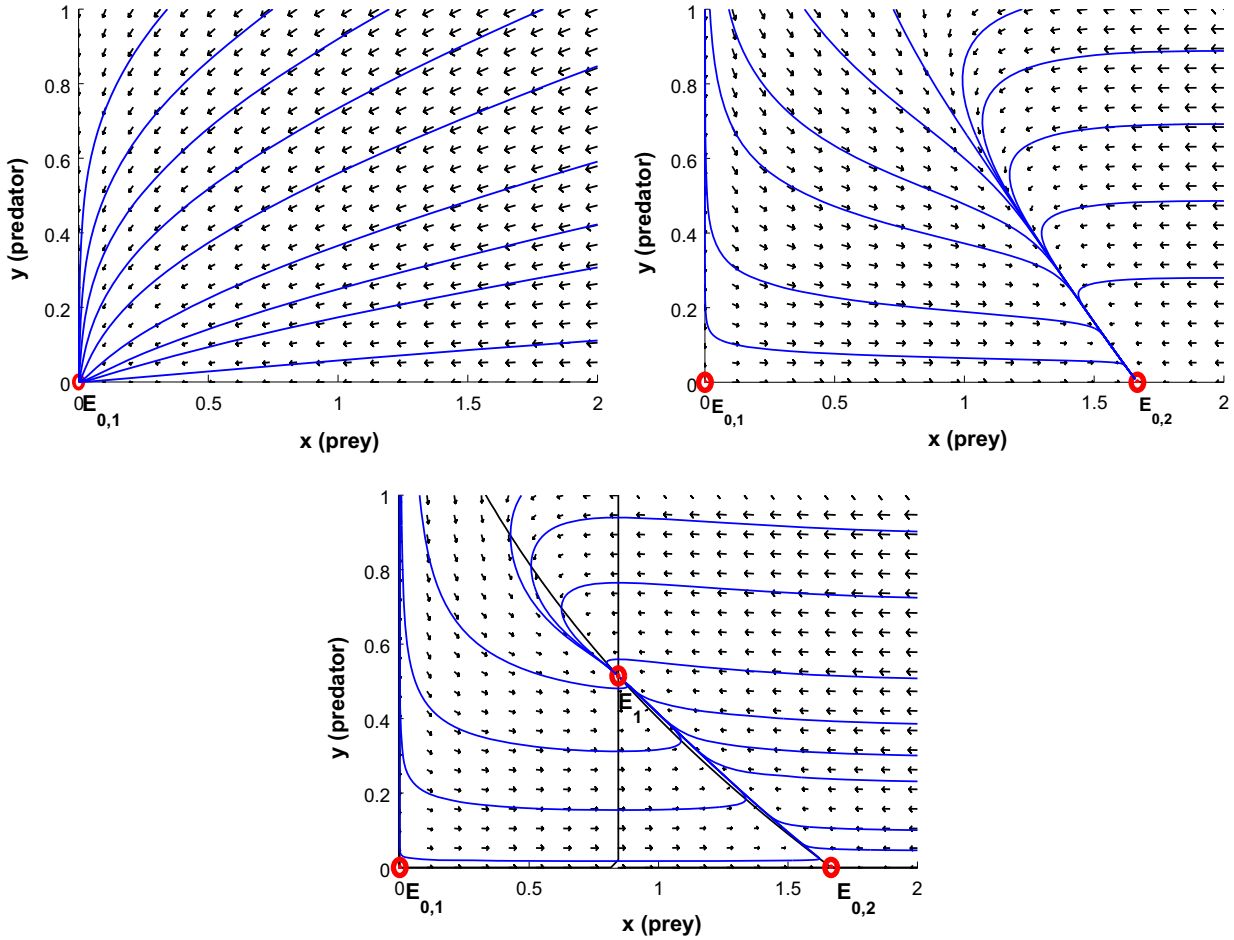

Fig. 4. Phase portraits of the predator density versus the prey density with various values of T and η. Units for prey and predator densities are dimensionless as described in Eq. (17). In each case, extirpation or coexistence equilibria are globally asymptotic stable (GAS). (top left) Extirpation equilibrium $E_{0,1}=(0,0)$ is GAS with $T=0.5$ and $\eta=1$. (top right) Extinction equilibrium $E_{0,2}=(1.67,0)$ is GAS with $T=0.2$ and $\eta=7$. (bottom) Coexistence equilibrium $E_1=(0.84,0.51)$ is GAS with $T=0.2$ and $\eta=3$. The other parameters for these three panels are the same as those in Fig. 3. Circles indicate equilibrium points.

half saturation constant η is large. In this scenario, the system has no interior equilibrium (i.e., both species cannot coexist) even though the toxin level T is low. In the bottom panel of Fig. 4, both species are able to coexist at interior equilibrium because the predation benefits the predator but is not too harmful to the prey when the toxin level T is low.

Fig. 5 shows that the both species coexist but the population levels oscillate periodically around the unstable interior equilibrium E_1. With limit-cycle oscillations, Fig. 5 clearly illustrates that the prey is reduced to extremely low levels yet recovers while the predator remains above a certain level even at the lowest prey population level.

In the previous section, we proved that E_2 is always an unstable saddle point when system has two interior equilibria E_1 and E_2. Figs. 6 and 7 show that system has two alternative stable states (bistability) when both interior equilibria E_1 and E_2 exist. The initial conditions determine which steady state the system will tend towards. The stable manifolds of the unstable interior equilibrium E_2 indicate the edges of the basin of attraction for each steady state. The bistability shown by Fig. 6 means that either the prey excludes the predator or both species coexist at the interior equilibrium E_1 depending on the initial population levels.

Fig. 7 shows another type of bistability. That is, system has two alternative stable states: either the prey excludes the predator or both species coexist but with oscillating population levels. When both species coexist but with oscillating population levels, both equilibria E_1 and E_2 are unstable. The system will tend towards a stable limit cycle only when the initial population fall in a small domain which is the basin of attraction of the limit cycle.

6. Effects of toxin on population dynamics

The goal of this section is to study how the balance of classical predator–prey dynamics will change as the concentration of a toxin increases from zero to higher level. To do so, we first present the results of classical predator–prey dynamics associated with our toxin-dependent predator–prey dynamics. We then plot bifurcation dynamics for the toxin-dependent system by regarding the external toxin level as a bifurcation parameter. The bifurcation figures will clearly illustrate how the external toxin changes the long-term asymptotic behavior of the prey and the predator.

6.1. A traditional predator–prey system

If there is no toxin ($T=0$), then system (20) reduces to the following prey–predator system:

$$\frac{dx}{dt}=\left(\frac{1}{1+x}-m_1\right)x-\frac{xy}{\eta+x},$$

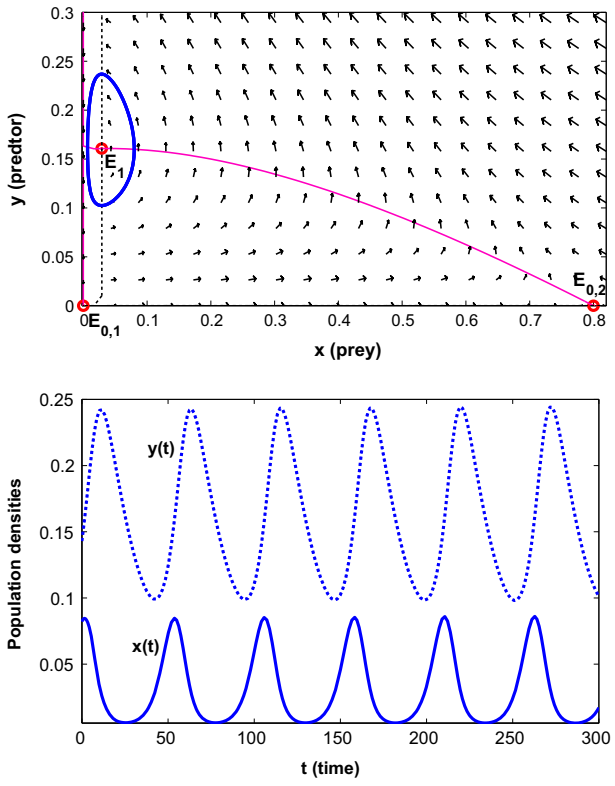

Fig. 5. System shows globally stable limit cycle. (top) Phase portraits of the predator density versus the prey density. (bottom) Solution curves (solid curve represents the prey density and dashed curve is the predator density). System has only one coexistence equilibrium $E_1=(0.028, 0.16)$ which is unstable spiral source, both boundary equilibria $E_{0,1}=(0,0)$ and $E_{0,2}=(0.80, 0)$ are unstable saddle points. Circles indicate equilibrium points. The parameters $T=0.1$, $\eta=0.4$, $m_1=0.4$, other parameters are the same as those in Fig. 3.

$$\frac{dy}{dt}=\frac{\beta_1 xy}{\eta+x}-m_2 y. \tag{29}$$

Regarding the existence and stability of the system (29), we have the following results:

Lemma 6.1. *Let* $0<m_1<1$ *and* $m_2<\beta_1$.

(1) *The boundary equilibrium* $E_{0,2}=(1/m_1-1, 0)$ *exists.* $E_{0,2}$ *is globally asymptotically stable if* $\eta>\frac{(1-m_1)(\beta_1-m_2)}{m_1 m_2}$.

(2) *If* $\eta<\frac{(1-m_1)(\beta_1-m_2)}{m_1 m_2}$, *then system (29) has only one interior equilibrium:*

$$E_1=\left(\frac{m_2\eta}{\beta_1-m_2}, \frac{\eta\beta_1[(1-m_1)(\beta_1-m_2)-m_1 m_2\eta]}{(\beta_1-m_2)(\beta_1-m_2+m_2\eta)}\right).$$

Assume that the interior equilibrium E_1 *exists, then* E_1 *is globally asymptotically stable if either* $\eta\geq 1$ *or both the conditions* $0<\eta<1$ *and* $\frac{(1-\eta)(\beta_1-m_2)^2}{(\beta_1-m_2+m_2\eta)^2}<m_1$ *are satisfied.*

We interpret the mathematical results in Lemma 6.1 as follows. First of all, the condition $0<m_1<1$ means that the loss rate of the prey biomass due to death is less than its maximum gain rate. If this condition is violated then both populations are extirpated. The condition $m_2<\beta_1$ means that the loss rate of the predator biomass is less than its maximum gain rate. If this condition is violated then the predator is extirpated and the system (29) reduces to a single species model:

(1) If the half-saturation constant is sufficiently large $\left(\eta>\frac{(1-m_1)(\beta_1-m_2)}{m_1 m_2}\right)$ (i.e., the capture efficiency is sufficiently low, assuming that the handling time is constant), then the prey-only equilibrium $E_{0,2}$ is stable, which means that the prey persists and the predator is eventually extirpated.

(2) Combining the conditions of existence and stability of coexistence equilibrium E_1, we find that both the species coexist in the following two scenarios:

(i) Both populations coexist at the equilibrium E_1 when the half-saturation constant is relatively large $\left(1\leq\eta<\frac{(1-m_1)(\beta_1-m_2)}{m_1 m_2}\right)$ (i.e., the capture efficiency is relatively low) and the mortality rate of the predator is sufficiently low $(m_2<(1-m_1)\beta_1)$. This is because if $1<\frac{(1-m_1)(\beta_1-m_2)}{m_1 m_2}$, which is equivalent to $m_2<(1-m_1)\beta_1$, then both populations are able to coexist if the condition $1\leq\eta<\frac{(1-m_1)(\beta_1-m_2)}{m_1 m_2}$ is also satisfied.

(ii) Both populations coexist at the equilibrium E_1 if the half-saturation constant is sufficiently small $(0<\eta<1)$ (i.e., the capture efficiency is sufficiently high) and the prey has an intermediate mortality rate $\left(\frac{(1-\eta)(\beta_1-m_2)^2}{(\beta_1-m_2+m_2\eta)^2}<m_1<\frac{\beta_1-m_2}{\beta_1-m_2+m_2\eta}\right)$. This is because we can equivalently rewrite the condition of the existence of E_1, $\eta<\frac{(1-m_1)(\beta_1-m_2)}{m_1 m_2}$, as $m_1<\frac{\beta_1-m_2}{\beta_1-m_2+m_2\eta}$, then both populations are able to coexist at E_1 if both conditions $0<\eta<1$ and $\frac{(1-\eta)(\beta_1-m_2)^2}{(\beta_1-m_2+m_2\eta)^2}<m_1<\frac{\beta_1-m_2}{\beta_1-m_2+m_2\eta}$ are satisfied.

Lemma 6.2. *If* $0<\eta<1$ *and* $m_1<\frac{(1-\eta)(\beta_1-m_2)^2}{(\beta_1-m_2+m_2\eta)^2}$, *then the system has a coexistence equilibrium* E_1 *which is unstable, and the system (29) possesses a unique limit cycle which is stable.*

Lemma 6.2 implies that both species coexist, but their densities fluctuate periodically if the half-saturation constant is sufficiently small $(0<\eta<1)$ (i.e., the capture efficiency is sufficiently high) and the mortality rate of the prey is sufficiently low $\left(m_1<\frac{(1-\eta)(\beta_1-m_2)^2}{(\beta_1-m_2+m_2\eta)^2}\right)$.

The stable limit cycle in Lemma 6.2 means that the prey and the predator coexist, but their densities fluctuate periodically. Similar to most standard predator–prey system, system (29) possesses three possible globally asymptotic stable state: prey only, coexistence at an equilibrium point, and coexistence at a limit cycle.

6.2. Dependence of stable population density on external toxin

In what follows, we consider how different toxin concentrations in the aquatic environment affect the predator–prey dynamics. To this end, we turn to the toxin-dependent system (20) and analyze the sensitivity of asymptotically stable states (equilibria) with respect to toxin level T. This sensitivity analysis illustrates how the stable densities of prey and predator vary when the toxin level in the environment increases from zero to a higher level. Mathematically, this can be done by treating stable equilibria (including the stable prey and predator densities) as a function of T, then calculating the rate of change of stable prey and predator densities with respect to T (see Appendix F).

We know from Table 2 and Theorem 4.2 that system (20) has a stable prey-only equilibrium $E_{0,2}=(x_0, 0)$ if external toxin levels are sufficiently high. The results of our sensitivity analysis imply that the prey density x_0 decreases as the toxin level T increases.

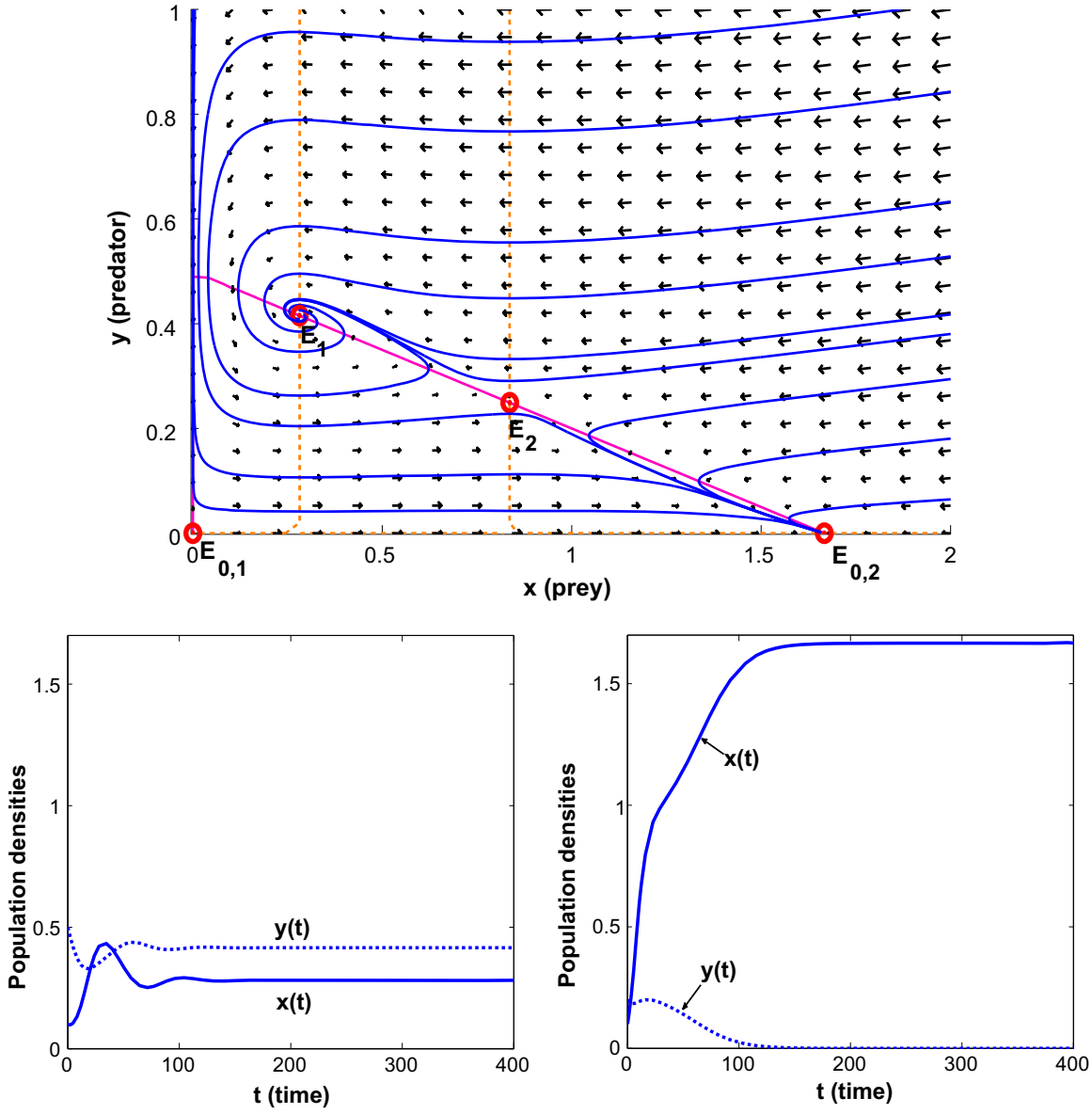

Fig. 6. System shows bistability with a locally stable coexistence equilibrium E_1 and a locally stable extirpation equilibrium $E_{0,2}$. The trajectories either converge to E_1 or converge to $E_{0,2}$. (top row) Phase portraits of the predator density versus the prey density. (bottom row) Solution curves. The solution with initial point $(0.1, 0.2)$ converges to E_1 (bottom left). The solution with initial point $(0.1, 0.5)$ converges to $E_{0,2}$ (bottom right). The system has two coexistence equilibria $E_1 = (0.28, 0.42)$ which is stable spiral node and $E_2 = (0.84, 0.25)$ which is an unstable saddle point. Boundary equilibrium $E_{0,1} = (0, 0)$ is an unstable saddle point. Boundary equilibrium $E_{0,2} = (1.67, 0)$ is stable node. Circles indicate equilibrium points. The parameters $\eta = 1$, other parameters are the same as those in Fig. 3.

That is, high concentrations of toxin in the environment are always harmful to the prey.

If the external toxin levels are sufficiently low, say $T < \min\{T_0^*, T_1^*, T_2^*\}$ (Table 2), and the half-saturation constants satisfy certain conditions (Table 2 and Theorem 4.3), then the system has a stable coexistence equilibrium $E_1 = (x_1, y_1)$. For this scenario, our analysis shows that y_1 is always a decreasing function of T, which means that toxin is always harmful to the predator, increasing toxin levels lead to decreasing predator density. However, toxin affects the asymptotic prey density in a different way: x_1 increases as the toxin level T increases from 0 to $\min\{T_0^*, T_1^*, T_2^*\}$ until the system shifts from the stable state of coexistence to prey-only state when the toxin level reaches the threshold value $\min\{T_0^*, T_1^*, T_2^*\}$. This threshold value determines whether a given toxin level is beneficial or harmful to the prey. The bifurcation dynamics shown in Fig. 8 in the next subsection illustrates our results of asymptotic analysis regarding the relationship between the stable population density and the toxin level in the environment.

6.3. Bifurcation dynamics

To further understand the effects of the toxin on predator–prey dynamics, next we plot the bifurcation dynamics of the system with respect to the toxin concentration T. In particular, we choose a set of parameters such that both species coexist at an interior equilibrium or limit cycle when there is no toxin ($T=0$). We then examine how these stable population densities will vary as T increases from zero to higher concentration.

Figs. 8–11 illustrate that the toxin concentration in the environment affects the population dynamics in many different ways. In Fig. 8, when $T=0$, both species coexists at an interior equilibrium. As T increases but still at a low concentration, the prey benefits since the stable predator density decreases. That is,

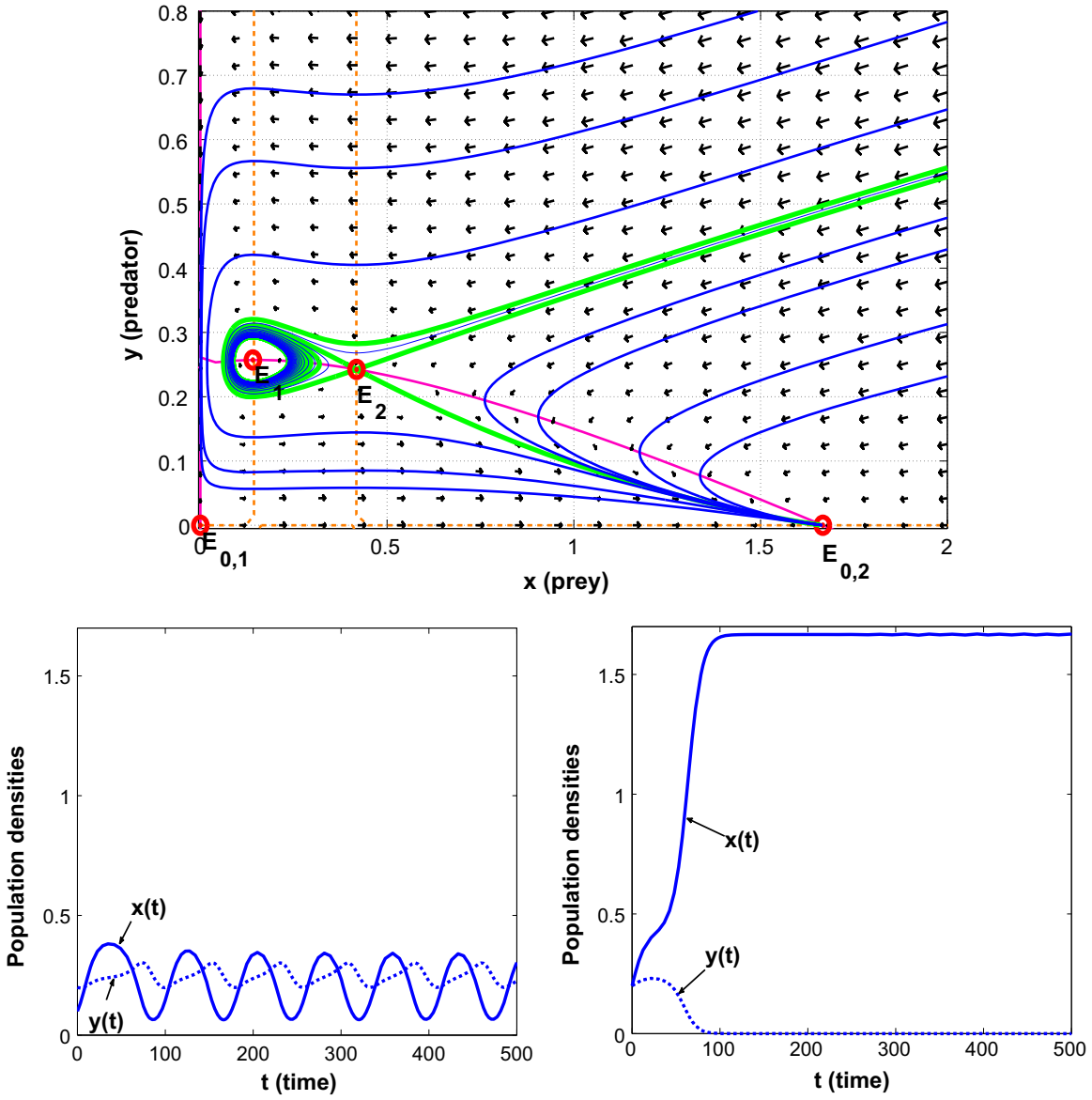

Fig. 7. System shows bistability with a locally stable limit cycle and a locally stable extirpation equilibrium $E_{0,2}$, The stable manifold of the limit cycle and the stable manifold of $E_{0,2}$ are depicted by bold curve. (top row) Phase portraits of the predator density versus the prey density. (bottom row) Solution curves. The solution with initial point $(0.1, 0.2)$, which belongs to the stable manifold of the limit cycle, oscillates periodically as shown by the limit cycle (bottom left). The solution with initial point $(0.2, 0.2)$, which is outside the limit cycle, converges to $E_{0,2} = (1.67, 0)$ (bottom right). System has two coexistence equilibria $E_1 = (0.14, 0.26)$ which is unstable spiral source and $E_2 = (0.42, 0.24)$ which is an unstable saddle point. Boundary equilibrium $E_{0,0} = (0, 0)$ is an unstable saddle point. Boundary equilibrium $E_{0,2} = (1.67, 0)$ is a stable node. Circles indicate equilibrium points. The parameters $\eta = 0.5$, other parameters are the same as those in Fig. 3.

contaminant effects on predators release the prey from predation, which lead to increased abundance of the prey. As T continues to increase, the stable prey level decreases and the predator is extirpated. Finally, if we increase T further, both species are extirpated. These results indicate that the low toxin concentration benefits the prey by reducing the predator abundance.

In Fig. 9, when $T=0$, both species coexists but oscillate around an unstable interior equilibrium. As T increases but still at a low concentration, population densities oscillate but with decreasing amplitudes until they reach a stable state at an interior equilibrium. As we continue to increase T further, similar dynamics to those in Fig. 8 are displayed. The unstable asymptotic behavior of the populations can be stabilized by increasing T. It seems that a high toxin environment excludes predator–prey cycles, which can be a disaster for the persistence of a predator–prey.

Figs. 10 and 11 show that the populations have alternative stable states over a certain range of T. In Fig. 10, the types of stable states vary in order as T increases. when $T=0$, both species coexist at an interior equilibrium. As T increases but still at low concentration, it benefits the prey since the stable predator density decreases. As we continue to increase T, the population densities tend to move to alternative stable states: either to a prey-only state or coexistence at an interior equilibrium. As T increases further, the coexistence state disappears and the population densities tend to a prey-only state. Finally, if we increase T even further, the stable prey density decreases until both species are extirpated.

In Fig. 11, both species coexists at a limit cycle when $T=0$. As T increases, population abundances continue to fluctuate but with decreasing amplitudes until they reach a bistable state: a stable limit cycle and a prey-only equilibrium. As we continue to increase T, the limit cycle disappears and another type of biostability appears: a stable coexistence equilibrium and a prey-only equilibrium. As T increases further, the coexistence state disappears and the population densities tend to the prey-only state. Finally, if we

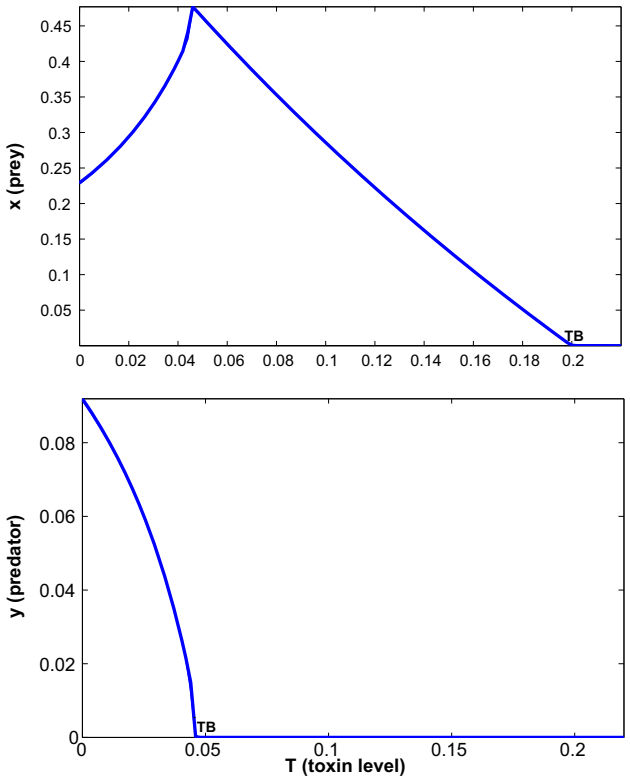

Fig. 8. Bifurcation diagram with respect to toxin level T for the case where both species coexist at interior equilibrium when $T=0$. TB: Transcritical bifurcation. Parameters: $m_1=0.6$, $\eta=0.2$, $\beta_1=0.75$, $m_2=0.4$, $k_1=1$, $k_2=1$, $\sigma_2=1$, $\beta_2=1$, $c=1$. Here $T_0^*=0.20$, $T_1^*=0.15$, $T_2^*=0.10$, $T_3^*=0.23$ (see Table 2).

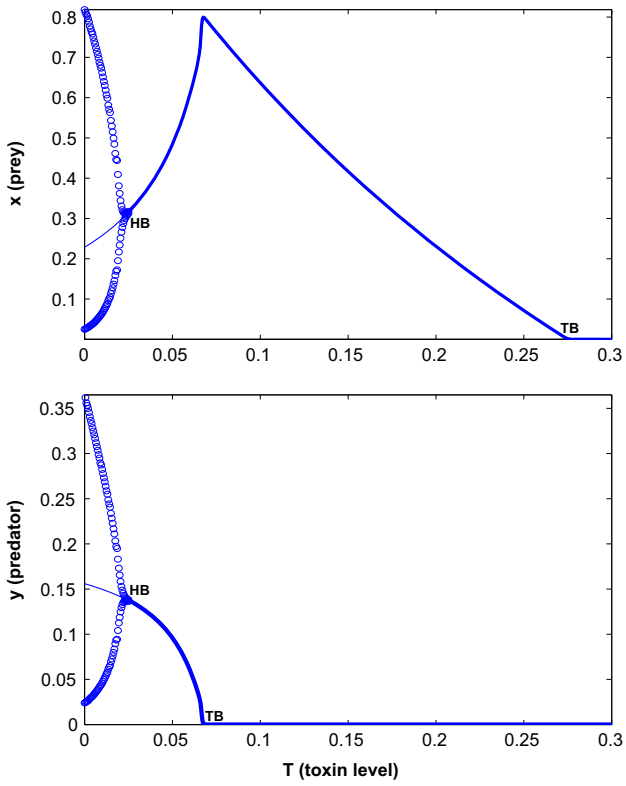

Fig. 9. Bifurcation diagram with respect to toxin level T for the case where both species coexist but oscillate around an unstable interior equilibrium when $T=0$. This shows highest and lowest values of x-coordinates and y-coordinate of stable limit cycles (open circles), x-coordinates and y-coordinates of unstable coexistence equilibria (thin solid curves), x-coordinates and y-coordinates of stable coexistence equilibria and prey-only equilibria (thick solid curves). HB: Hopf bifurcation, TB: Transcritical bifurcation. Parameters $m_1=0.45$, other parameters are the same as those in Fig. 8. Here $T_0^*=0.28$, $T_1^*=0.15$, $T_2^*=0.10$, $T_3^*=0.23$ (see Table 2).

increase T even further, the stable prey density decreases until both species are extirpated.

Figs. 8–11 highlight several key points: (1) High toxin concentration in the environment is harmful to both species, and it may lead to extirpation of both species. (2) The population dynamics are counter-intuitive when both the prey and the predator are exposed in an environment with low concentration of toxin. That is, low toxin concentration benefits the prey because the bioaccumulation of toxin in the predator reduces the predator abundance, which releases its prey from predation. (3) The amplitude of population oscillation around the unstable coexistence equilibrium can be reduced until it stabilizes at a coexistence equilibrium, as the toxin concentration increases. (4) Certain toxin levels may lead to more than one asymptotic population density of either the prey or the predator. In this scenario, the initial population density of the prey or the predator determines its eventual population density.

7. Discussion

Contamination by toxic pollutants is a significant problem in water management (Helmer and Hespanhol, 1997). The effect of a toxic contaminant can, in principle, be exerted on all levels of the biological hierarchy, from cells to organs to organisms to populations to entire ecosystems. Mathematical models are useful tools for evaluating the ecological significance of observed or predicted effects of toxic chemicals on individual organisms and population dynamics. Most toxin-dependent single-species models (e.g., Freedman and Shukla, 1991; Hallam and Clark, 1983; Hallam et al., 1983; Luna and Hallam, 1987; Thieme, 2003; Thomas et al., 1996; Huang et al., 2013) assume that populations take up contaminants from water and ignore bioaccumulation (contaminant uptake, excretion, and contaminant transfer through aquatic food chain) These single-species models cannot predict the effects of toxin on species interactions, nutrient cycling, or contaminant flow in aquatic systems.

Motivated by the fact that many aquatic organisms take up contaminants both from water and from food (their prey), we developed a toxin-dependent predator–prey model by assuming that the prey and the predator are exposed simultaneously to a toxin. Unlike those existing toxin-dependent food web models (e.g., Kooi et al., 2008; Garay-Narväez et al., 2013, 2014) which describe the interactions between populations, toxin in the populations, and toxin in the environment, our model focuses on the impact of toxin on the populations and ignores the influence of the population on the toxin in the environment. To facilitate model analysis, we approximated the model with a two dimensional system because population metabolism takes place over a much faster time scale than population growth does. We then analyzed the existence and stability of extirpation and coexistence equilibria based on the two dimensional system. The conditions that guarantee the existence and stability of equilibria provide meaningful biological interpretations. For instance, high toxin concentrations in the environment lead to the extirpation of prey and predators, and low toxin concentrations lead to the coexistence of both populations. However, intermediate toxin concentrations result in two alternative stable states: a prey-only equilibrium and coexistence of prey and predators. In this scenario, the initial conditions determine which steady state the populations will tend towards. The results of model analysis were then used to show all possible asymptotic behaviors of the system. To do this, we plotted a series of phase portraits to identify possible outcomes. These outcomes suggest that our toxin-dependent system has richer

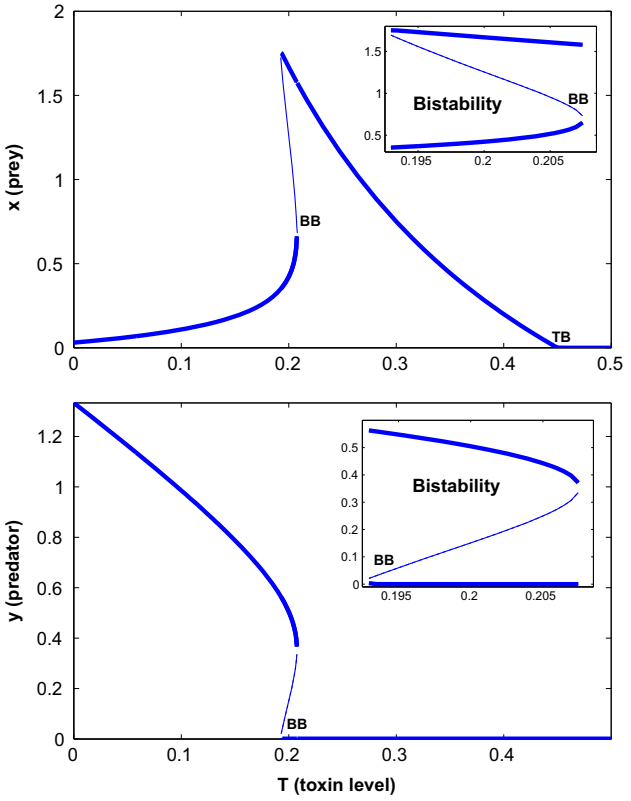

Fig. 10. Bifurcation diagram with respect to toxin level T. The system has two coexistence equilibria when T lies within a certain range. Stable equilibria (thick solid curves). Unstable equilibria (thin solid curves). BB: Backward bifurcation, TB: Transcritical bifurcation. Parameters: $\eta=1.5$, $\beta_1=1$, $m_1=0.1$, $m_2=0.02$, $k_1=1$, $k_2=0.2$, $\sigma_2=1$, $\beta_2=4$, $c=1.5$. Here $T_0^*=0.45$, $T_1^*=0.21$, $T_2^*=0.15$, $T_3^*=0.097$ (see Table 2). Note that the condition $\max\{T_2^*,T_3^*\}<\min\{T_0^*,T_1^*\}$ is satisfied, the system has two coexistence equilibria. When $0.193<T<0.208$, the system has bistability, which is highlighted at the top right corners of the panels.

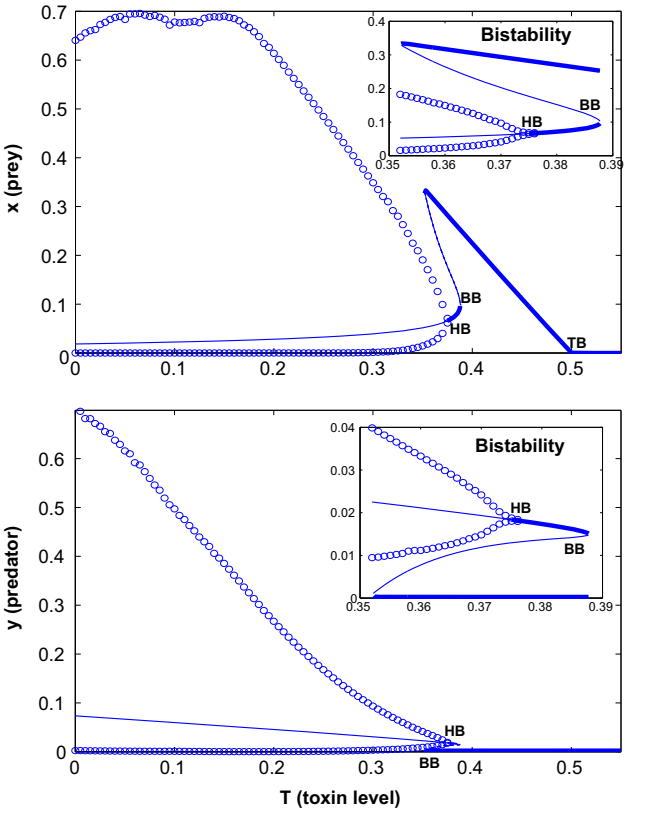

Fig. 11. Bifurcation diagram with respect to toxin level T. The system has two types of bistabilities. The highest and lowest values of x-coordinates and y-coordinate of stable limit cycles (open circles), x-coordinates and y-coordinates of unstable coexistence equilibria (thin solid curves), x-coordinates and y-coordinates of stable coexistence equilibria and prey-only equilibria (thick solid curves). HB: Hopf bifurcation, TB: Transcritical bifurcation, BB: Backward bifurcation. Parameters: $\eta=0.12$, $\beta_1=0.75$, $m_2=0.1$, $k_1=0.1$, $k_2=0.1$, $\sigma_2=1$, $\beta_2=2$, $c=0.5$. Here $T_0^*=0.50$, $T_1^*=0.39$, $T_2^*=0.31$, $T_3^*=0.21$ (see Table 2). Note that the condition $\max\{T_2^*,T_3^*\}<\min\{T_0^*,T_1^*\}$ is satisfied, the system has two coexistence equilibria. When $0.352<T<0.388$, the system has bistability, which is highlighted at the top right corners of the panels.

dynamics than traditional predator–prey system due to the existence of two interior equilibria and bistability.

Predator–prey interactions are one of the central themes in ecology (Matia and Alam, 2013). The dynamics of traditional predator–prey systems have been well documented (Cheng, 1981; Hsu, 1977; Hsu and Huang, 1995; Sugie et al., 1997). The main aim of the present study is to investigate how the balance of a traditional predator–prey system (without a toxin effect) will change when the prey and the predator are exposed in an aquatic environment where toxins may be present at low levels. To this end, we focused on bifurcation dynamics with toxin level as a bifurcation parameter. As shown in Figs. 8–11, our toxin-dependent model exhibits rich dynamics including transcritical, Hopf, and backward bifurcations. Our results imply that sublethal contaminant effects on predator–prey interactions can be counter-intuitive. That is, increased toxin level can have a positive effect on prey persistence, even though it has a negative effect on predator persistence. This is because the bioaccumulation of toxin in the predator reduces the predator abundance, which releases its prey from predation. In addition, our findings indicate that toxins may also reduce population variability by preventing populations from fluctuating around a coexistence equilibrium, which often occur in traditional predator–prey systems.

For model analysis, since the study of the linear stability of coexistence equilibria of four-dimensional system (18) is intractable, we mainly focused on local stable analysis of equilibria based on the quasi-steady system (20). However, it might be possible to study analytically the stability of the boundary equilibria of system (18) that correspond to the equilibria of the reduced system in rows A and B of Table 2. Moreover, as we observed in Section 5, the quasi-steady system (20) has several types of phase portraits, we believe that the global dynamics will provide more clear insights into the effects of a toxin on long-term behaviors, but this is a challenging task and is left for future work.

Species in different trophic levels may have different sensitivities to each toxin. We hope to encourage the connection of the model with data to other species and toxins of interest. The bifurcation analysis in Section 6.3 can provide threshold values of toxin concentration in the environment for the persistence of one or both species. The threshold value for shifting the system from one stable state to another can also be observed. This will help evaluate acute and chronic guideline developments for target species and chemicals.

Our model assumes that concentration of the toxin in the environment is a constant. In reality, the toxin concentration may vary over time (and space, if sediment and plant uptake and release are considered) due to a variety of factors. In addition, we have only considered the interaction between one predator species and one prey species. When toxins flow across multiple prey and predators, the outcome can be more complicated. Our model also assumes that the capture rate in Holling's type II function response is a constant. In practice, contaminant-induced changes in a population's behavior may also lead to abundance changes in prey and predator populations. For

example, the dynamics might be very different if predators prefer "toxic" prey (because they are slower, sicker, easier to catch) versus if they avoid toxic prey (because they taste bad or they know that the toxin is bad for them). Further consideration of these factors in the model framework is required to investigate this problem. We expect that the main results we obtained in this study are robust, even though the details will certainly change if we include these factors in the model.

In this paper, we develop a comprehensive framework for understanding impacts of toxins on multitrophic population dynamics. Although our toxin-dependent predator–prey system is developed based on an aquatic environment, the model and the results in this study are applicable to predator–prey systems in terrestrial ecosystems.

Acknowledgments

The authors wish to thank Caroline Bampfylde, Chris Powter, and Lewis Lab for fruitful discussions. The Oil Sands Research and Information Network, School of Energy and the Environment, University of Alberta provided funding for this work. We also received suggestions, input and initial direction from Alberta Environment and Sustainable Resource Development. H.W. gratefully acknowledge NSERC Discovery Grant. M.A.L. also gratefully acknowledges a Canada Research Chair and NSERC Discovery and Accelerator Grants.

Appendix A. Proof of Theorem 4.1

Proof. Positivity obviously holds for the system (18). Let $z(t)=\beta_1 x(t)+y(t)$ and differentiating z once yields

$$\begin{aligned}\frac{dz}{dt}&=\beta_1\left(\frac{\max\{0,1-u\}}{1+x}-k_1u-m_1\right)x\\&\quad-\beta_1\frac{xy}{\eta+x}+\frac{\beta_1 xy\max\{0,1-v\}}{\eta+x}\\&\quad-(k_2v+m_2)y\\&\le\beta_1-\beta_1m_1x-m_2y\\&\le\beta_1-\min\{m_1,m_2\}z,\end{aligned}\tag{30}$$

which implies

$$\limsup_{t\to\infty}z(t)\le\frac{\beta_1}{\min\{m_1,m_2\}}\quad\text{and}$$
$$z(t)\le\max\left\{\frac{\beta_1}{\min\{m_1,m_2\}},z(0)\right\}.\tag{31}$$

On the other hand, from the third equation of the system (18), we have

$$\epsilon\frac{du}{dt}\le T-u,\tag{32}$$

Similar to the argument on $z(t)$, we can conclude that

$$\limsup_{t\to\infty}u(t)\le T.\tag{33}$$

Thus, given $\delta>0$, there exists $t_0>0$ such that $u(t)<T+\delta$ for all $t>t_0$. Therefore, from the fourth equation of the system (18), we obtain

$$\epsilon\frac{dv}{dt}\le cT-\sigma_2v+\beta_2u\le cT+\beta_2(T+\delta)-\sigma_2v,\tag{34}$$

which indicates that $v(t)$ is also ultimately bounded.□

Appendix B. Argument about the assumptions (21)–(22)

Clearly, if $m_1\ge1$, then for any $x\ge0$ and $T\ge0$,

$$\frac{\max\{0,1-T\}}{1+x}-k_1T-m_1<\frac{1}{1+x}-m_1<1-m_1<0,$$

thus $\lim_{t\to\infty}x(t)=0$, which will lead to $\lim_{t\to\infty}y(t)=0$.

If $T\ge1$, then $\max\{0,1-T\}=0$, thus $\lim_{t\to\infty}x(t)=0$, $\lim_{t\to\infty}y(t)=0$.

Similarly, if $cT\ge\sigma_2$, then $\max\{0,1-cT/\sigma_2-\beta_2Tx/(\sigma_2(\eta+x))\}=0$, thus $\lim_{t\to\infty}y(t)=0$.

If $m_2>\beta_1$, then for any $x\ge0$ and $T\ge0$,

$$\frac{\beta_1x\max\left\{0,1-\frac{cT}{\sigma_2}-\frac{\beta_2T}{\sigma_2}\frac{x}{\eta+x}\right\}}{\eta+x}-k_2\left(\frac{cT}{\sigma_2}+\frac{\beta_2T}{\sigma_2}\frac{x}{\eta+x}\right)-m_2<\beta_1-m_2<0,$$

thus, $\lim_{t\to\infty}y(t)=0$, and the system (20) reduces to a single species model.

Appendix C. Existence of equilibria

The prey x-nullclines

$$x=0,\quad y=\frac{f(x)}{\varphi(x)},\tag{35}$$

and the predator y-nullclines are

$$g(x)=0\quad\text{or}\quad y=0.\tag{36}$$

From the intersections of the nullclines, we find that the system has only one extinction equilibrium $E_{0,1}=(0,0)$ if $T\ge(1-m_1)/(k_1+1):=T_0^*$, and the system has an extinction equilibrium $E_{0,1}$ and a prey-only equilibrium $E_{0,2}=(x_0,0)$ if $T<T_0^*$ with $x_0=(1-T)/(k_1T+m_1)-1$.

The interior equilibria (coexistence equilibria) can be found by setting

$$g(x)=0\quad\text{and}\quad y=\frac{f(x)}{\varphi(x)}>0.\tag{37}$$

Noticing that $\varphi(x)$ is an increasing positive function on $(0,\infty)$, we require

$$f(x)=\left(\frac{1-T}{1+x}-k_1T-m_1\right)x>0,\tag{38}$$

that is, $T<T_0^*$ and $0<x<(1-T)/(k_1T+m_1)-1:=F(\varphi)=x_0$. The second condition is equivalent to

$$\varphi(x)<\varphi(x_0).\tag{39}$$

Also, if $\varphi(x)\ge(\sigma_2-cT)/\beta_2T$, then $\max\{0,1-cT/\sigma_2-\beta_2T\varphi(x)/\sigma_2\}=0$. In this case, $g(x)<0$. Hence, we require

$$\varphi(x)<\frac{\sigma_2-cT}{\beta_2T}.\tag{40}$$

When (40) holds, function $g(x)$ becomes

$$\begin{aligned}g(x)&=\beta_1\varphi(x)\left(1-\frac{cT}{\sigma_2}-\frac{\beta_2T}{\sigma_2}\varphi(x)\right)-\frac{k_2cT}{\sigma_2}-\frac{k_2\beta_2T}{\sigma_2}\varphi(x)-m_2\\&=-\frac{1}{\sigma_2}\left[\beta_1\beta_2T(\varphi(x))^2-(\beta_1(\sigma_2-cT)-k_2\beta_2T)\varphi(x)+k_2cT+m_2\sigma_2\right].\end{aligned}\tag{41}$$

Therefore, system (23) has coexistence equilibrium if and only if the quadratic equation with respect to $\varphi:=\varphi(x)$

$$\beta_1\beta_2T\varphi^2-[\beta_1(\sigma_2-cT)-k_2\beta_2T]\varphi+k_2cT+m_2\sigma_2=0\tag{42}$$

has at least one positive root which satisfies

$$\varphi<\min\left\{\frac{\sigma_2-cT}{\beta_2T},\varphi(x_0)\right\}.\tag{43}$$

Let

$$\Delta := [\beta_1(\sigma_2 - cT) - k_2\beta_2 T]^2 - 4\beta_1\beta_2 T(k_2 cT + m_2\sigma_2). \tag{44}$$

Notice if $\Delta \geq 0$, the quadratic equation (42) has either two positive roots (when $\beta_1(\sigma_2 - cT) - k_2\beta_2 T > 0$) or two negative roots (when $\beta_1(\sigma_2 - cT) - k_2\beta_2 T < 0$).

Thus, we require that (42) has two positive roots. We also find that (42) has two positive roots

$$\varphi_{1,2} = \frac{\beta_1(\sigma_2 - cT) - k_2\beta_2 T \mp \sqrt{\Delta}}{2\beta_1\beta_2 T}, \tag{45}$$

if and only if the following condition holds:

$$\beta_1(\sigma_2 - cT) - k_2\beta_2 T > 2\sqrt{\beta_1\beta_2 T(k_2 cT + m_2\sigma_2)}. \tag{46}$$

Next, we equivalently rewrite the condition (46) into a restriction condition with respect to T. Firstly, the condition (46) implies that $\beta_1(\sigma_2 - cT) - k_2\beta_2 T > 0$, which is equivalent to

$$T < \frac{\beta_1\sigma_2}{\beta_1 c + k_2\beta_2}. \tag{47}$$

Secondly, if we introduce a function G with respect to T,

$$G(T) = \beta_1(\sigma_2 - cT) - k_2\beta_2 T - 2\sqrt{\beta_1\beta_2 T(k_2 cT + m_2\sigma_2)}. \tag{48}$$

Then G is a decreasing function of T. Solving $G(T) = 0$, we can get a threshold value of T, which is

$$T = \frac{\beta_1\sigma_2(\beta_1 c + k_2\beta_2 + 2\beta_2 m_2) - \beta_1\sigma_2\sqrt{4\beta_2(\beta_1 c + \beta_2 m_2)(m_2 + k_2)}}{(\beta_1 c - k_2\beta_2)^2} := T_1^*. \tag{49}$$

Clearly, $G(\beta_1\sigma_2/(\beta_1 c + k_2\beta_2)) < 0$, since $G(T^*) = 0$ and $G(\cdot)$ is a decreasing function, so $T^* < \beta_1\sigma_2/(\beta_1 c + k_2\beta_2)$.

Therefore, a combination of (47) and (49) yields that the condition (46) is equivalent to

$$T < T_1^*. \tag{50}$$

We now require φ_1 and (or) φ_2 satisfy the condition (43). We notice that

$$\varphi_1 < \varphi_2 < \frac{\sigma_2 - cT}{\beta_2 T}. \tag{51}$$

In fact, we have

$$\begin{aligned} \varphi_2 < \frac{\sigma_2 - cT}{\beta_2 T} &\Leftrightarrow \frac{\beta_1(\sigma_2 - cT) - k_2\beta_2 T + \sqrt{\Delta}}{2\beta_1\beta_2 T} < \frac{\sigma_2 - cT}{\beta_2 T} \\ &\Leftrightarrow \sqrt{\Delta} < \beta_1(\sigma_2 - cT) + k_2\beta_2 T \\ &\Leftrightarrow \Delta < (\beta_1(\sigma_2 - cT) + k_2\beta_2 T)^2 \\ &\Leftrightarrow -4\beta_1\beta_2 T\sigma_2(k_2 + m_2) < 0, \end{aligned} \tag{52}$$

which is true. Thus, the existence of coexistence equilibrium depends on whether or not $\varphi_{1,2} < \varphi(x_0)$.

Noticing that $0 < \varphi(x_0) = x_0/(\eta + x_0) < 1$ and φ_1 and φ_2 do not depend on η (see Eq. (45)), we can choose appropriate η such that $\varphi_{1,2} < \varphi(x_0)$ if $\varphi_{1,2} < 1$.

From (45), we find that $\varphi_1 < 1 < \varphi_2$ if

$$T < \frac{(\beta_1 - m_2)\sigma_2}{\beta_1\beta_2 + \beta_1 c + k_2\beta_2 + k_2 c} := T_2^*, \tag{53}$$

and $\varphi_1 < \varphi_2 < 1$ if

$$T > \max\{T_2^*, T_3^*\}, \tag{54}$$

where

$$T_3^* = \frac{\beta_1\sigma_2}{\beta_1 c + k_2\beta_2 + 2\beta_1\beta_2}. \tag{55}$$

Therefore, if $T < \min\{T_0^*, T_1^*, T_2^*\}$ and $\eta < x_0/\varphi_1 - x_0$, then system (23) has only one coexistence equilibrium $E_1 = \left(x_1, \frac{f(x_1)}{\varphi(x_1)}\right)$, where x_1 is given by $\varphi_1 = \varphi(x_1)$. More precisely, since $\varphi_1 = x_1/(\eta + x_1)$, we have $x_1 = \eta\varphi_1/(1 - \varphi_1)$.

If $T_3^* < \min\{T_0^*, T_1^*\}$, then system (23) has two coexistence equilibria E_1 and $E_2 = \left(x_2, \frac{f(x_2)}{\varphi(x_2)}\right)$ with $x_2 = \eta\varphi_2/(1 - \varphi_2)$ when $T_3^* < T < \min\{T_0^*, T_1^*\}$ and $\eta < x_0/\varphi_2 - x_0$.

Appendix D. Proof of Theorem 4.2

Proof. At $E_{0,1}$, where both prey and predator are extinct, the Jacobian is

$$J(E_{0,1}) = \begin{pmatrix} f'(0) & -\varphi(0) \\ g'(0) & g(0) \end{pmatrix} = \begin{pmatrix} 1 - T - k_1 T - m_1 & 0 \\ 0 & -\frac{k_2 cT}{\sigma_2} - m_2 \end{pmatrix} \tag{56}$$

and the eigenvalues are the components on the diagonal:

$$\lambda_1 = 1 - T - k_1 T - m_1, \quad \lambda_2 = -\frac{k_2 cT}{\sigma_2} - m_2. \tag{57}$$

If $k_1 T + m_1 + T > 1$, then $E_{0,1}$ is a stable node because both eigenvalues of $J(E_0)$ are negative. Moreover, only the boundary equilibrium $E_{0,1}$ is feasible when $k_1 T + m_1 + T > 1$. Because solutions are bounded, solutions must converge to $E_{0,1}$. If $k_1 T + m_1 + T < 1$, then $E_{0,1}$ is a saddle point because the two real eigenvalues are of opposite sign.

The Jacobian at $E_{0,2}$, where only the prey survives, is

$$J(E_{0,2}) = \begin{pmatrix} f'(x_0) & -\varphi(x_0) \\ 0 & g(x_0) \end{pmatrix} \tag{58}$$

and the eigenvalues are

$$\lambda_1 = f'(x_0) = \frac{(k_1 T + m_1)(T + k_1 T + m_1 - 1)}{1 - T}, \quad \lambda_2 = g(x_0). \tag{59}$$

The condition of the existence of $E_{0,1}$, $T + k_1 T + m_1 < 1$, implies that $\lambda_1 < 0$. Thus, the stability of $E_{0,1}$ can be determined by the sign of eigenvalue of $g(x_0)$. That is, $E_{0,1}$ is a stable (unstable) node (saddle point) if $g(x_0) < (>) 0$.

Next, we investigate the condition $g(x_0) < 0$ further under which $E_{0,1}$ is a stable node. Let $\varphi_0 = x_0/(\eta + x_0)$, using (41) and (42) we find that $g(x_0) < 0$ is equivalent to

$$\beta_1\beta_2 T\varphi_0^2 - [\beta_1(\sigma_2 - cT) - k_2\beta_2 T]\varphi_0 + k_2 cT + m_2\sigma_2 := F(\varphi_0) > 0 \tag{60}$$

Using the same discriminant Δ as in (44), we consider the following cases:

(i) If $\Delta < 0$, then $F(\varphi_0)$ represents a parabola which opens upward and does not intersect φ_0-axis, then $F(\varphi_0) > 0$ for any φ_0. From the discussion about the existence of equilibria (see Appendix C), we can easily find that $\Delta < 0$ is equivalent to

$$T_1^* < T < T_4^*, \tag{61}$$

where

$$T_4^* := \frac{\beta_1\sigma_2(\beta_1 c + k_2\beta_2 + 2\beta_2 m_2) + \beta_1\sigma_2\sqrt{4\beta_2(\beta_1 c + \beta_2 m_2)(m_2 + k_2)}}{(\beta_1 c - k_2\beta_2)^2} \tag{62}$$

(ii) If $\Delta > 0$ and $\beta_1(\sigma_2 - cT) - k_2\beta_2 T < 0$ (i.e., $T > \beta_1\sigma_2/(\beta_1 c + k_2\beta_2)$), then $F(\varphi_0)$ represents a parabola which opens upward and intersects half φ_0-axis, then $F(\varphi_0) > 0$ since $\varphi_0 > 0$. Again, from the discussion about the existence of equilibria (see Appendix), we know that $\Delta > 0$ is equivalent to $T < T_1^*$ and

$T_1^* < \beta_1\sigma_2/(\beta_1 c + k_2\beta_2)$. Therefore, the condition $\Delta > 0$ contracts the condition $\beta_1(\sigma_2 - cT) - k_2\beta_2 T < 0$.

(iii) If $\Delta > 0$ and $T < \beta_1\sigma_2/(\beta_1 c + k_2\beta_2)$ (note that $\Delta > 0$ is equivalent to $T < T_1^*$ and $T_1^* < \beta_1\sigma_2/(\beta_1 c + k_2\beta_2)$), then $F(\varphi_0)$ represents a parabola which opens upward and intersects positive φ_0-axis, $F(\varphi_0) = 0$ has two positive roots φ_1 and φ_2 ($\varphi_1 < \varphi_2$). Thus, $F(\varphi_0) > 0$ when $\varphi_0 < \varphi_1$ (i.e., $\eta > x_0/\varphi_1 - x_0$) or $\varphi_0 > \varphi_2$ (i.e., $\eta < x_0/\varphi_2 - x_0$).

From (i)–(iii), we conclude that the prey-only equilibrium $E_{0,2}$ is locally asymptotically stable if one of the following conditions is satisfied: (1) $T_1^* < T < T_4^*$, (2) $T < T_1^*$ and $\eta > x_0/\varphi_1 - x_0$, (3) $T < T_1^*$ and $\eta < x_0/\varphi_2 - x_0$. Note that the condition plays a role only when the conditions $\max\{T_2^*, T_3^*\} < \min\{T_0^*, T_1^*\}$ and $\max\{T_2^*, T_3^*\} < T < \min\{T_0^*, T_1^*\}$ are satisfied (see Section 3.1.1).□

Appendix E. Proof of Theorem 4.3

Proof. At coexistence equilibria E_i ($i = 1, 2$), where both prey and predator coexist, the Jacobian is

$$J(E_i) = \begin{pmatrix} f'(x_i) - \varphi'(x_i)\dfrac{f(x_i)}{\varphi(x_i)} & -\varphi(x_i) \\ g'(x_i)\dfrac{f(x_i)}{\varphi(x_i)} & 0 \end{pmatrix} \tag{63}$$

and the characteristic equation is

$$\lambda^2 - \left[f'(x_i) - \varphi'(x_i)\frac{f(x_i)}{\varphi(x_i)}\right]\lambda + g'(x_i)f(x_i) = 0. \tag{64}$$

For the equilibrium E_1, simple calculation gives

$$g'(x_1) = -\frac{1}{\sigma_2}[2\beta_1\beta_2 T\varphi(x_1) - \beta_1(\sigma_2 - cT) + k_2\beta_2 T)]\varphi'(x_1) = \frac{\sqrt{\Delta}\varphi'(x_1)}{\sigma_2} > 0. \tag{65}$$

Since the quantities $g'(x_1)$ and $f(x_1)$ are positive, the Routh–Hurwitz criterion guarantees that equilibria E_1 are stable if

$$f'(x_1) - \varphi'(x_1)\frac{f(x_1)}{\varphi(x_1)} < 0. \tag{66}$$

Note that

$$f'(x_1) - \varphi'(x_1)\frac{f(x_1)}{\varphi(x_1)} = \varphi(x_1)\left(\frac{f(x_1)}{\varphi(x_1)}\right)', \tag{67}$$

and $\varphi(x_1) > 0$, the (66) is equivalent to

$$\left(\frac{f(x_1)}{\varphi(x_1)}\right)' < 0. \tag{68}$$

simple calculation yields

$$\left(\frac{f(x_1)}{\varphi(x_1)}\right)' = \frac{(1-T)(1-\eta)}{(1+x_1)^2} - (k_1 T + m_1). \tag{69}$$

Clearly, if $\eta > 1$, then condition (68) is satisfied, E_1 is stable. If $\eta < 1$, then (68) is equivalent to

$$k_1 T + m_1 < \frac{(1-T)(1-\eta)}{(1+x_1)^2}. \tag{70}$$

Therefore, E_1 is stable either $\eta \geq 1$ or both conditions $0 < \eta < 1$ and $k_1 T + m_1 < \frac{(1-T)(1-\eta)}{(1+x_1)^2}$ are satisfied.□

Appendix F

Analytical calculations on the sensitivity of stable population density on toxin

If the system (23) has a stable prey-only equilibrium $E_{0,2} = (x_0, 0)$ with $x_0 = (1-T)/(k_1 T + m_1) - 1$, then the stable prey density decreases as the toxin level T increases because x_0 is a decreasing function of T.

If the condition

$$\left(\frac{f(x_1)}{\varphi(x_1)}\right)' < 0 \tag{71}$$

is satisfied (here $'$ denote the derivative with respect to x), then the system (23) has a stable coexistence equilibrium $E_1 = (x_1, y_1)$ with $x_1 = \frac{\eta\varphi_1}{1-\varphi_1}$ and $y_1 = \frac{f(x_1)}{\varphi(x_1)} = \frac{f(x_1)}{\varphi_1}$, where φ_1 is given by the following quadratic equation (see (42)):

$$\beta_1\beta_2 T\varphi_1^2 - [\beta_1(\sigma_2 - cT) - k_2\beta_2 T]\varphi_1 + k_2 cT + m_2\sigma_2 = 0. \tag{72}$$

Differentiating both sides of the above equation with respect to T, we have

$$\frac{\partial\varphi_1}{\partial T} = \frac{-(\beta_1\beta_2\varphi_1^2 + k_2\beta_2\varphi_1 + \beta_1 c\varphi_1 + k_2 c)}{2\beta_1\beta_2 T\varphi_1 + k_2\beta_2 T + \beta_1 cT - \beta_1\sigma_2}. \tag{73}$$

Applying (44) to the above equation, we have

$$\frac{\partial\varphi_1}{\partial T} = \frac{-(\beta_1\beta_2\varphi_1^2 + k_2 c + \varphi_1 k_2\beta_2 + \varphi_1\beta_1 c)}{-\sqrt{\Delta}} > 0. \tag{74}$$

Therefore,

$$\frac{\partial x_1}{\partial T} = \frac{\partial x_1}{\partial\varphi_1}\frac{\partial\varphi_1}{\partial T} > 0, \tag{75}$$

since $\partial x_1/\partial\varphi_1 > 0$ is obvious from $x_1 = \eta\varphi_1/(1-\varphi_1)$.

That is, if the system stabilizes at the coexistence equilibrium $E_1 = (x_1, y_1)$, then the stable prey density always increases as the toxin level T increases:

$$\frac{\partial y_1}{\partial T} = \left(\frac{f(x_1)}{\varphi(x_1)}\right)'\frac{\partial x_1}{\partial T} < 0. \tag{76}$$

That is, if the system stabilizes at the coexistence equilibrium $E_1 = (x_1, y_1)$, then the stable predator density always decreases as the toxin level T increases.

References

Abnoos, H., Fereidoni, M., Mahdavi-Shahri, N., Haddad, F., Jalal, R., 2013. Developmental study of mercury effects on the fruit fly (*Drosophila melanogaster*). Interdiscip. Toxicol. 6 (1), 34–40.

Arnot, J.A., Gobas, F.A., 2004. A food web bioaccumulation model for organic chemicals in aquatic ecosystems. Environ. Toxicol. Chem. 23, 2343–2355.

Bartell, S.M., Pastorok, R.A., Akcakaya, H.R., Regan, H., Ferson, S., Mackay, C., 2003. Realism and relevance of ecological models used in chemical risk assessment. Hum. Ecol. Risk Assess. 9, 907–938.

Bax, N.J., 1998. The significance and prediction of predation in marine fisheries. ICES J. Mar. Sci. 55, 997–1030.

Canadian Council of Ministers of the Environment, 2003a. Canadian water quality guidelines for the protection of aquatic life: Guidance on the Site-Specific Application of Water Quality Guidelines in Canada: Procedures for Deriving Numerical Water Quality Objectives.

Canadian Council of Ministers of the Environment, 2003b. Canadian water quality guidelines for the protection of aquatic life: inorganic mercury and methylmercury. In: Canadian environmental Quality Guidelines, 1999. Canadian Council of Ministers of the Environment, Winnipeg, Manitoba. 6 pp. ⟨http://ceqg-rcqe.ccme.ca/download/en/191⟩ (Last accessed November 21, 2014).

Cheng, K.S., 1981. Uniqueness of a limit cycle for a predator–prey system. SIAM J. Math. Anal. 12 (4), 541–548.

Depew, D.C., Burgess, N.M., Anderson, M.R., Baker, R., Bhavsar, S.P., Bodaly, R.A., Eckley, C.S., Evans, M.S., Gantner, N., Graydon, J.A., Jacobs, K., LeBlanc, J.E., Louis, V.L.S., Campbell, L.M., 2013. An overview of mercury concentrations in freshwater fish species: a national fish mercury dataset for Canada. Can. J. Fish. Aquat. Sci. 70, 1–16.

Eisler, R., 1987. Mercury Hazards to Fish, Wildlife and Invertebrates: A Synoptic Review. U.S. Fish and Wildlife Service, Laurel, Maryland. Biological Report 85 (1.10). Contaminant Hazard Reviews Report No. 10. 63 pp. ⟨http://www.pwrc.usgs.gov/eisler/CHR_10_Mercury.pdf⟩ (Last accessed November 21, 2014).

Elliott, J.M., 1981. A quantitative study of the life cycle of the net-spinning caddis *Philopotamus montanus* (Trichoptera: Philopotamidae) in a Lake District stream. J. Anim. Ecol. 50, 867–883.

Elliott, J.M., 1982. A quantitative study of the life cycle of the case-building caddis *Odontocerum albicorne* (Trichoptera: Odontoceridae) in a Lake District stream. Freshw. Biol. 12, 241–255.

Freedman, H.I., Shukla, J.B., 1991. Models for the effect of toxicant in single-species and predator–prey systems. J. Math. Biol. 30, 15–30.

Galic, N., Hommen, U., Baveco, J.H., van den Brink, P.J., 2010. Potential application of population models in the European ecological risk assessment of chemicals. II: review of models and their potential to address environmental protection aims. Integr. Environ. Assess. Manag. 6, 338–360.

Garay-Narväez, L., Flores, J.D., Arim, M., Ramos-Jiliberto, R., 2014. Food web modularity and biodiversity promote species persistence in polluted environments. Oikos 123, 583–588.

Garay-Narväez, L., Flores, J.D., Arim, M., Ramos-Jiliberto, R., 2013. The more polluted the environment, the more important biodiversity is for food web stability. Oikos 122 (55), 1247–1253.

Gilpin, M.E., Ayala, F.J., 1973. Global models of growth and competition. Proc. Natl. Acad. Sci. USA 70, 3590–3593.

Gobas, F.A.P.C., de Wolf, W., Burkhard, L.P., Verbruggen, E., Plotzke, K., 2009. Revisiting bioaccumulation criteria for POPs and PBT assessments. Integr. Environ. Assess. Manag. 5, 624–637.

Hallam, T.G., Clark, C.E., 1983. Effect of toxicants on populations: a qualitative approach. I. Equilibrium environmental exposure. Ecol. Model. 18, 291–304.

Hallam, T.G., Clark, C.E., Jordan, G.S., 1983. Effect of toxicants on populations: a qualitative approach. II. First order kinetics. J. Math. Biol. 18, 25–37.

Helmer, R., Hespanhol, I., 1997. Water Pollution Control—A Guide to the Use of Water Quality Management Principles. Published on behalf of the United Nations Environment Programme, the Water Supply &Sanitation Collaborative Council and the World Health Organization by E. & F. Spon. WHO/UNEP.

Hildrew, A.G., Rüdiger, W., 1992. The briefly colonial life of hatchlings of the net-spinning caddisfly *Plectrocnemia conspersa*. J. N. Am. Benthol. Soc. 11, 60–68.

Hsu, S.B., 1977. On global stability of a predator–prey system. Math. Biosci. 39, 1–10.

Hsu, S.B., Huang, T.W., 1995. Global stability for a class of predator–prey system. SIAM J. Appl. Math. 55, 763–783.

Holling, C.S., 1959. The components of predation as revealed by a study of small mammal predation of the Europe pine sawfly. Can. Entomol. 91, 293–320.

Huang, Q., Parshotham, L., Wang, H., Bampfylde, C., Lewis, M.A., 2013. A model for the impact of contaminants on fish population dynamics. J. Theor. Biol. 334, 71–79.

Jensen, P.D., Sorensen, M.A., Walton, W.E., Trumble, J.T., 2007. Lethal and sublethal responses of an aquatic insect *Culex quinquefasciatus* (Diptera: Culicidae) challenged with individual and joint exposure to dissolved sodium selenate and methylmercury chloride. Environ. Toxicol. 22 (3), 287–294.

Kelly, B.C., Ikonomou, M.G., Blair, J.D., Morin, A.E., Gobas, F.A.P.C., 2007. Food web-specific biomagnification of persistent organic pollutants. Science 317, 236–239.

Kidd, K.A., Blanchfield, P.J., Mills, K.H., Palace, V.P., Evans, R.E., 2007. Collapse of a fish population after exposure to a synthetic estrogen. Proc. Natl. Acad. Sci. USA 104 (21), 8897–8901 ⟨http://www.pnas.org/cgi/reprint/0609568104v1⟩ (Last accessed November 21, 2014).

Kooi, B.W., Bontje, D., van Voorn, G.A.K., Kooijman, S.A.L.M., 2008. Sublethal toxic effects in a simple aquatic food chain. Ecol. Model. 212, 304–318.

Kooijman, S.A.L.M., Bedaux, J.J.M., 1996. The Analysis of Aquatic Toxicity Data. VU University Press, Amsterdam.

Kot, M., 2001. Elements of Mathematical Ecology. Cambridge University Press, Cambridge.

Luna, J.T., Hallam, T.G., 1987. Effect of toxicants on populations: a qualitative approach. IV. Resource–consumer–toxiocant models. Ecol. Model. 35, 249–273.

Matia, S.N., Alam, S., 2013. Prey-predator dynamics under herd behavior of prey. Univ. J. Appl. Math. 1 (4), 251–257.

McElroy, A.E., Barron, M.G., Beckvar, N., Driscoll, S.B.K., Meador, J.P., Parkerton, T.F., Preuss, T.G., Steevens, J.A., 2010. A review of the tissue residue approach for organic and organometallic compounds in aquatic organisms. Integr. Environ. Assess. Manag. 7, 50–74.

Miller, F., Janszen, P.D., 2000. Haber's rule: A special case in a family of curves relating concentration and duration of exposure to a fixed level of response for a given endpoint. Toxicology 149, 21–34.

Mackay, D., Fraser, A., 2000. Bioaccumulation of persistent organic chemicals: mechanisms and models. Environ. Pollut. 110, 375–391.

Mathew, R., McGrath, J.A., Toro, D.M.D., 2008. Modeling polycyclic aromatic hydrocarbon bioaccumulation and metabolism in time-variable early life-stage exposures. Environ. Toxicol. Chem. 27, 1515–1525.

Pastorok, R.A., Akcakaya, H.R., Regan, H., Ferson, S., Bartell, S.M., 2003. Role of ecological modeling in risk assessment. Hum. Ecol. Risk Assess. 9, 939–972.

Pastorok, R.A., Bartell, S.M., Ferson, S., Ginzburg, L.R., 2001. Ecological Modeling in Risk Assessment: Chemical Effects on Populations, Ecosystems, and Landscapes. Lewis Publishers, Boca Raton, FL, USA.

Polis, G.A., Myers, C.A., Holt, R.D., 1989. The ecology and evolution of intraguild predation—potential competitors that eat each other. Annu. Rev. Ecol. Syst. 20, 297–330.

Sandheinrich, M.B., Wiener, J.G., 2011. Methylmercury in freshwater fish recent advances in assessing toxicity of environmentally relevant exposures. In: Beyer, W.N., Meador, J.P. (Eds.), second ed. CRC Press, Boca Raton, Florida, pp. 169–190.

Sugie, J., Kohno, R., Miyazaki, R., 1997. On a predator–prey system of Holling type. Proc. Am. Math. Soc. 125, 2041–2050.

Thomann, R.V., 1989. Bioaccumulation model of organic chemical distribution in aquatic food chains. Environ. Sci. Technol. 23, 699–707.

Thieme, H.R., 2003. Mathematics in Population Biology. Princeton Series in Theoretical and Computational Biology.

Thomas, D.M., Snell, T.W., Jaffar, S.M., 1996. A control problem in a polluted environment. Math. Biosci. 133, 139–163.

U.S. National Archives and Records Administration, 2013. Code of Federal Regulations, Title 40- Protection of Environment, Appendix A to Part 423-126 Priority Pollutants.

Wente, S.P., 2004. A Statistical Model and National Dataset for Partitioning Fish-tissue Mercury Concentration Between Spatio-temporal and Sample characteristic Effects. United States Geological Survey Scientific, Reston, Virginia. Investigation Report 2004-5199. 21 pp.

Willis, L.D., Hendricks, A.C., 1992. Life history, growth, survivorship, and production of Hydropsyche slossonae in Mill Creek, Virginia. J. N. Am. Benthol. Soc. 11, 293–303.

Xie, L., Flippin, J.L., Deighton, N., Funk, D.H., Dickey, D.A., Buchwalter, D.B., 2009. Mercury(II) bioaccumulation and antioxidant physiology in four aquatic insects. Envioron. Sci. Technol. 43, 934–940.